UNIVERSITÀ DEGLI STUDI DI PADOVA

DIPARTIMENTO DI BIOLOGIA

Corso di Laurea magistrale in Marine Biology

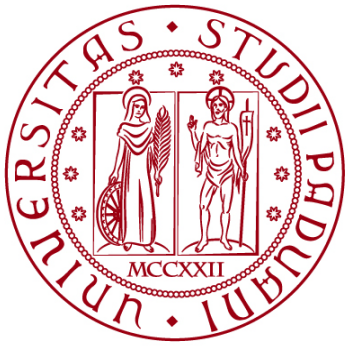

TESI DI LAUREA

Boreogadus saida physiological responses under future ocean acidification and warming scenarios

Relatore: Prof.ssa Chiara Papetti
Dipartimento di Biologia (DiBio)

Correlatore*: Dott. Magnus Lucassen
Istituto Alfred Wegener (AWI)

Laureanda: Erica Difronzo

ANNO ACCADEMICO 2023/2024

Table of Contents

1 Abstract

Mitochondria play a key role in cellular metabolism and aerobic energy production, furthermore modifications in mitochondrial functions have been demonstrated to be involved in the acclimation of ectothermal fish. The present study wants to address the potential consequences of future climate change scenarios of ocean warming and acidification on Polar cod (*Boreogadus saida*), a key species in the Arctic Circle. In response to a combination of four different temperatures (0, 3, 6, 8 °C) and two pCO_2 (390 and 1170 ppm), the aim of the present study is to analyse the number of mitochondria per cell, the expression of crucial enzymes in mitochondrial metabolism (CS, COX1, COX2, COX4, ND1, ND6, and ATP6), along with the enzymes capacity. The DNA content as well as DNA expression was not affected by the treatments, whereas only ND1 showed an effect caused by pCO_2 at 8 °C. The mitochondrial number per cell was not significantly affected by the treatments, though a mitochondrial rearrangement in its structure and functions seems to have occurred. RNA content strongly decreased with high temperature, as well as COX4 and CS mRNA expression. As for mitochondrial encoded genes, mRNA expression of ND6 and ATP6 was significantly downregulated by temperature. Most evident and intense effect were observed with proteins. Protein content steeply decreased with increasing temperatures, while COX capacity significantly increased with raising temperature and pCO_2. CS capacity along with F_OF_1 ATP synthase protein expression significantly decreased due to high temperature, contrasting with the pattern of COX. Nonetheless, the drastic fall of the temperature coefficient (Q_{10}) in both CS and COX is a sign of the loss of sensitivity of these key enzymes when acclimated to 8 °C. Further analyses are needed to complete the picture, however, is clear that temperature is the main driver of these changes, while pCO_2 acclimation seems to have a more marginal effect.

2 Sommario

I mitocondri svolgono un ruolo chiave nel metabolismo cellulare e nella produzione di energia, inoltre è stato dimostrato che modifiche nelle funzioni mitocondriali sono coinvolte nell'acclimatazione degli organismi ectotermi. Nel presente studio si vogliono indagare le potenziali conseguenze degli scenari futuri di riscaldamento e acidificazione degli oceani sul Merluzzo Polare (*Boreogadus saida*), una specie chiave del Circolo Polare Artico. In risposta a una combinazione di quattro diverse temperature (0, 3, 6, 8 °C) e due concentrazioni di CO_2 (390 e 1170 ppm), l'obiettivo è quello di analizzare il numero di mitocondri per cellula, l'espressione di enzimi cruciali nel metabolismo mitocondriale (CS, COX1, COX2, COX4, ND1, ND6 e ATP6), e l'attività enzimatica. Il contenuto e l'espressione del DNA non sono stati influenzati dall'acclimatazione ai vari trattamenti; tuttavia, è stato rilevato un effetto indotto dalla pressione parziale di anidride carbonica ($PaCO_2$) su ND1. Il numero di mitocondri per cellula non è stato influenzato in modo significativo dai trattamenti, sebbene sembri essersi verificato un riarrangiamento nella struttura e nelle funzioni mitocondriali. Il contenuto di RNA è stato fortemente diminuito dall'elevata temperatura, così come l'espressione dell'mRNA di COX4 e CS. Per quanto riguarda i geni del genoma mitocondriale, l'espressione dell'mRNA di ND6 e ATP6 è risultata significativamente ridotta a seguito dell'incremento della temperatura. L'effetto più evidente è stato osservato con l'analisi delle proteine. Il contenuto proteico è diminuito bruscamente con l'aumento della temperatura, mentre l'attività enzimatica di COX è aumentata significativamente con l'aumento della temperatura e della $PaCO_2$. Viceversa, l'attività enzimatica di CS e l'espressione proteica della ATP sintasi F_OF_1 è diminuita significativamente a causa dell'alta temperatura, in contrasto con l'andamento di COX. Tuttavia, il drastico calo del coefficiente di temperatura (Q_{10}) sia per CS che per COX rappresenta un sintomo della perdita di sensibilità di questi enzimi chiave quando acclimatati a 8 °C. Ulteriori analisi sono necessarie per completare il quadro; nondimeno, è chiaro che la temperatura rappresenti il principale motore di questi cambiamenti, mentre la $PaCO_2$ sembrerebbe avere un ruolo secondario.

3 Introduction

3.1 Climate change impacts on the ocean

Anthropogenic climate change is indubitably damaging marine ecosystems, approaching irreversible scenarios, such as the retreat of glaciers, permafrost thawing and global sea level rise, with human activities being the main driver of these changes. Global surface temperature has increased by 1.1 °C above 1850-1900 in the years 2011-2020 and the main cause can be traced back to the continuous human-caused emission of greenhouse gases (GHGs; IPCC, 2023). First GHG for excellence, carbon dioxide (CO_2), has increased in concentration from 280 parts per million (ppm) in pre-industrialized atmosphere (Watson et al. 1990) to 410 ppm in 2019 (IPCC, 2023), followed by methane (CH_4), which increased from 800 parts per billion (ppb) in 1860 (Fang et al. 2013) to 1866 ppb in 2019 (IPCC, 2023). Through all this time the hydrosphere has been storing most of the greenhouse gases released, but above all, the ocean has absorbed approximately a third of all human CO_2 emissions since industrialization (Sabine et al. 2004), as well as a consistent part of the thermic energy released, leading to thermal expansion and sea-level rise (Zanna et al. 2019). Specifically, the upper ocean (0-700 m) temperature has increased since the 1970's (IPCC, 2023), and particular attention has been given to the sea surface temperature (SST) and its anomalies. SST tend to vary seasonally and geographically, but anomalies of multi-decadal warmer SSTs, caused by greenhouse gases, has been registered (Bulgin et al. 2020). Anomalies of SST are indeed strongly coupled with ocean circulation changes and low- to midlatitude air-sea interactions (Zanna et al. 2019). One of the most known SST anomalies is El Nino Southern Oscillation (ENSO), a fluctuation between unusual warm (El Nino) and cold (La Nina) conditions in the tropical Pacific, which occurs every 2 to 7 years (McPhaden et al. 2006). Furthermore, SST anomalies registered in the ENSO tropical Pacific area exhibit decadal variability, cooling in the 1980's and warming in the 1990's. Moreover, in the decade 2000-2009 SST anomalies displayed less change than any other decades registered, coinciding with low ENSO variability in the same period, whereas in the decade 2010-2018 the strongest warming trend was registered (Bulgin et al. 2020).

Over the past 2 million years CO_2 concentrations has never been higher than present ones (IPCC, 2023) and this is not affecting ocean temperature alone but is causing ocean acidification too. The world´s ocean represent the largest sink for the CO_2, buffering the release of GHG. When the ocean uptakes CO_2, the concentration of bicarbonate (HCO_3^-) and hydrogen ion (H^+) increases, thus lowering the pH, given

that $pH = -\log_{10}[H^+]$. The buffer capacity of the ocean holds on the availability of calcite ($CaCO_3$), which derives from shells and skeletons of marine organisms, such as plankton, corals, and coralline algae (Doney et al. 2009). A study from Jiang et al. (2019) measured the surface pH of the oceans (adjusted for the year 2000), having the lowest pH value in the eastern Pacific one, whereas the Arctic Ocean showed the largest variability in surface water pH, with a global average of 8.07 ± 0.02, which is about ~0.11 ± 0.03 units more acidic than 1770.

3.2 Concept of oxygen- and capacity- limited thermal tolerance (OCLTT)

Marine animals are mostly ectothermal meaning that they have to cope with the pervasive environmental temperature. Temperature is the most important abiotic factor as it affects all biological processes directly. The physiological mechanisms causing heat or chill death have been studied for over a century to identify the temperature-associated death, yet a comprehensive mechanism-based understanding of this process was mostly left out. Accordingly, the concept of oxygen- and capacity- limited thermal tolerance (OCLTT) proposes a molecular to whole animal approach to investigate the thermal constraints on the capacity of oxygen supply to the organism in relation to oxygen demand (Pörtner et al. 2017). OCLTT could be considered as an extension of the concepts of critical thermal maximum (CT_{max}) and lethal temperature causing 50 % mortality (LT_{50}). According to OCLTT, all organisms live within a range of temperature which is optimal for all their needs and are limited by pejus (which means “turning worse”), critical, and denaturation temperatures (Pörtner & Farrell 2008; Figure 3.1). Aerobic scope is defined as the absolute difference between the maximum and the “resting” rates of aerobic metabolism that an animal can achieve (Gleeson 1981). As temperature goes beyond pejus limits, for both sides, aerobic scopes, and oxygen supply decrease. As temperature rises or decreases approaching a critical limit, all spontaneous activity stops entailing food uptake. Beyond critical temperatures, extreme hypoxia overtakes (Pörtner 2002 a). Additional factors like increasing pCO_2 (hypercapnia) or environmental hypoxia are thought to narrow the thermal window. Moreover, different life stages exhibit specific susceptibilities with respect to temperature with eggs, early larvae and spawners being most sensitive (Pörtner et al. 2017; Figure 3.1).

The concept of OCLTT can be extremely helpful for a better understanding of the species responses to climate change. Species that are constrained in a narrow thermal window, which reduces their functions, face a threat to their survival. For

example, following the increase in water temperature in the German Wadden Sea, the abundance of common eelpout *Zoarces viviparus* decreased over the 35-year period from 1954 to 1989, reflecting a high mortality in hot summers (Pörtner & Knust 2007). Even though individuals may survive non-lethal thermal constraints, the resulting reduction in available energy will endanger reproduction and thus population survival (Pörtner et al. 2017). The width of the thermal window differs between ectotherms from different climate zones being the largest in species from temperate zones, facing seasonal and even daily fluctuations in temperature, therefore designated as eurythermal, and the smallest in cold-adapted species from high latitudes (being stenothermal) (Figure 3.1). On top, eurythermal species usually possess high capacities for thermal acclimation upon environmental change. Such differences between windows may lead to shifts in spatial or temporal overlaps, causing previously matched species interactions to go out of phase, and hence leading to a change in food availability (Pörtner & Farrell 2008).

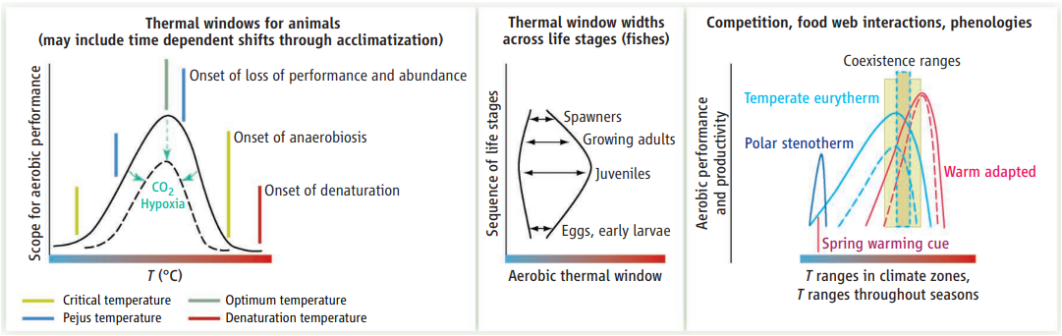

Figure 3.1 **Temperature effects on aquatic animals.** On the **left** are displayed the thermal windows of aerobic performance, with optimal temperature, limited by pejus, critical and denaturation temperatures, at which tolerance becomes increasingly passive and time limited. In the **middle** are displayed positions and widths of windows on the temperature scale shift with life stages. The **right** window displays a possible representation of thermal windows of species with different biogeographies, where thermal windows could still overlap (Pörtner & Farrell 2008).

3.3 Mitochondrial quantification

Mitochondria play a key role in cellular metabolism and aerobic energy production, with the generation of ATP through oxidative phosphorylation, along with the regulation of intracellular signalling cascades, generation of reactive oxygen species (ROS), fatty acids β-oxidation, and so on. (Popov 2020). Considering the importance of the mitochondrial role in so many aspects of cellular homeostasis, any perturbation or stress to the organelle's function may trigger cell death, and this has been demonstrated to bring diverse mitochondrial-associated pathologies in mammals. Therefore, cells have evolved efficient repair mechanisms as well as

turnover pathways, like mitophagy, to ultimately solve potentially damaging perturbances (reviewed by Ploumi et al. 2017). Although mitochondria display an impressive metabolic as well as genetic autonomy, many of the functions are run by both mitochondrial and cellular physiology. As instance, mitochondrial biogenesis requires the presence of proteins expressed by both mitochondrial and nuclear DNA (nucDNA) (reviewed by Tronstad et al. 2014). Usually, mitochondrial biogenesis in mammals is an adaptive response to metabolic changes and energy depletion, such as endurance exercise, cold exposure, caloric restriction, as well as oxidative stress during cell division and differentiation (reviewed by Tronstad et al. 2014). It becomes clear that any mitochondrial content variation, when measured, could show an additional perspective on the organism reaction to any source of stress.

The first method ever used to determine mitochondrial fractional area was based on electron transmission microscope (TEM), a stereological method which allows the acquisition of information about three-dimensional, microscopical structures through two-dimensional sections, as defined by Gundersen et al. (1988). However, TEM technique is time consuming, and some laboratory may lack this microscope, therefore mitochondrial content can be measured indirectly through biomarkers, such as mitochondrial proteins, lipids, enzyme activities, and DNA (Larsen et al. 2012). The most common biomarker utilized in mitochondrial content measurement is the mitochondrial DNA (mtDNA). mtDNA quantification usually requires RealTime Polymerase chain reaction (PCR) and can be performed with or without a standard curve. In the case of relative quantification, the cycle threshold (C_T) values of the samples are compared to those of the standard curve, to determine mitochondrial DNA copy number per PCR reaction (Read et al. 2021; Rooney et al. 2015). Otherwise, mitochondrial content can be measured without the construction of standard curve, but from the variation of mtDNA copy number relative to nucDNA through PCR absolute quantification (Otten et al. 2016; Rooney et al. 2015).

3.4 Cold adaptation in ectotherms

As ectothermic animals acclimatize to cold temperatures, they experience a deceleration in all cellular processes. To maintain a functional balance between energy allocation and demand, the organism compensates by adjusting physiological processes, such as the velocity of enzymatic reactions, the rates of diffusion, the membrane fluidity and flexibility (Hochachka & Somero 2002; Somero 2004). A key role in this process is represented by the mitochondria, crucial in the acclimatization to seasonal cold, as well as in the evolutionary cold adaptation

of marine ectotherms (Lucassen et al. 2006). As temperature decreases, the organism needs to increase ATP production, to keep the rate of the biochemical reaction stable. A common strategy is to increase the concentration of aerobic metabolic enzymes per gram of tissue, which often coincides with an increase in percentage of cell volume displaced by mitochondria (O'Brien 2011). Accordingly, enzymes like citrate synthase (CS), implied in the citric acid cycle, and cytochrome *c* oxidase (COX), a component of the oxidative electron transport chain, can turn into great sentinels to monitor the long-term acclimation of fish mitochondria and limitation to temperature (Hardewig et al. 1999; Lannig et al. 2003; Lucassen et al. 2006). In the study conducted by Lucassen et al. 2006, two populations of cod *Gadus morhua* sampled along a latitudinal cline, showed tissue-specific increments in CS and COX activities, when acclimatized to low temperatures. Specimens from the cold-adapted population responded to larger extent emphasising the role of mitochondrial adjustment for cold adaptation. Furthermore, shifts in the ratio of CS over COX in the liver indicate the use of different fuels along the thermal window with lipids preferred in the cold. Similar, the hepatosomatic index (HSI), an indicator of the relative liver size, increased upon cold acclimation, which promotes an increased use of lipids in the cold, as the liver stores large quantities of lipids in gadid fish (Lucassen et al. 2006).

Besides, marine ectotherms specialize to different thermal windows (Figure 3.1) and the adaptation they undergo to the environmental conditions are reflected at the molecular and physiological level. Warm-bodied animals tends to achieve a high performance with lower mitochondrial densities than cold-adapted species, which have developed high mitochondrial densities and lipid depots (Pörtner 2002 a). For instance, the mitochondrial volume density in Antarctic fish (29-31 %) is much higher than those in Mediterranean fish (8-13 %) (Johnston et al. 1998). Nevertheless, the functional capacity of single mitochondria was found to be lower in the cold-adapted species, indicating diverse constraints and demands for specific adjustments of mitochondrial functions.

3.5 Mitochondrial sensitivity to climate change in ectotherms

Temperature represents a critical abiotic factor which shapes the distribution and the abundance of species. However, the mechanisms at the base of organismal thermal limits are still poorly understood. There is some evidence for a direct causal connection between failure of mitochondrial respiratory capacity (measured *in vitro*) and whole-organism critical thermal limits, although is not sufficient to support a functional link between the two. The most compelling evidence seen so

far, which represent a link between mitochondrial and whole-organismal thermal performance, regards the ATP synthesis (reviewed by Chung & Schulte 2020). Nevertheless, evident signs of heat stress endured by an organisms can be clearly seen through mitochondrial responses. A study conducted on two wrasses, the temperate *Notolabrus fucicola* and the tropical *Thalassoma lunare*, indicated that some forms of cardiac mitochondrial dysfunctions occurred even below the temperature of heart failure and that the tropical *T. lunare* was closer to heart failure than its equivalent *N. fucicola*, and as such would be the most susceptible to rising sea water temperatures (Iftikar et al. 2014). In fact, warm-adapted species may be less tolerant to heat than cold-adapted species (Stillman & Somero 2000). Mitochondrial enzyme capacities can be affected as well by rising temperature, thus many studies on fish highlighted a suppressed citrate synthase (CS) activity and cytochrome *c* oxidase (COX) activity as well, even if to a lesser extent (Lannig et al. 2003, 2005; Leo et al. 2020; Windisch et al. 2011).

Most of the studies so far focuses on the effects of high temperature on mitochondrial functions, yet ocean acidification can seriously impair the long-term survival of ectotherm organisms. As instance, after a warm-hypercapnia exposure of the Antarctic fish *Notothenia rossii*, the activity of CS and COX in liver decreased (Strobel et al. 2013). Moreover, long term exposure to elevated CO_2 levels of the Mediterranean species *Sparus aurata* led to a drop in CS activity in white and red muscles (Michaelidis et al. 2007).

Other studies highlighted the synergistic effect of elevated CO_2 concentrations, when associated to warm acclimation. In a study conducted by Howald et al. (2019), the exposure of European seabass (*Dicentrarchus labrax* L.) to high pCO_2 resulted in no changes, except when associated to long-term warming, whose effects were amplified by pCO_2 exposure. Moreover, in Atlantic cod (*G. morhua*) *in vivo* mitochondrial respiration was depressed when exposed to combined high temperature and high pCO_2 (Leo et al. 2017).

3.6 Polar cod *Boreogadus saida* (Lepechin, 1774)

Polar cod (*Boreogadus saida* (Lepechin, 1774)), sometimes also addressed as Arctic cod, is a major species in the Arctic (Welch et al. 1992). With a length of around 300 mm (Scott & Scott 1988), Polar cod is a small fish which can live up to 7 years (Hop et al. 1997). *B. saida* presents a circumpolar distribution above the Arctic Circle (Cohen et al. 1990), and specifically larvae and juveniles can be found under or near ice cover (Bouchard & Fortier 2011; David et al. 2016). Polar cod represents a key-role in the Arctic marine food web, as it acts as energy transformer between

its small preys (such as *Calanus* spp. and *Themisto* spp.) and big predators like marine mammals and seabirds (Welch et al. 1992).

Polar cod, as most high Arctic stenotherms, are associated with low temperatures, such as between -1.5 and 2 °C in the Barents Sea (Loeng 1991) and between 0-2 °C in the Beaufort Sea (Crawford et al. 2012). Nevertheless, a preferred temperature range between 3 and 6 °C was found in growth performance studies (Schurmann & Christiansen 1994; Kunz et al 2016), being still much narrower compared to eurythermal species, including its congener *G. morhua*, from temperate zones.

3.6.1 Effects of climate change on Polar cod

Ecosystems characterized by low resilience, such as polar ones, are most likely facing irreversible adverse impact following a 1.5 °C increase in global temperature (IPCC, 2023). Accordingly, cold-adapted organisms adapted to such environments would inevitably suffer consequences. Several studies have demonstrated Polar cod sensitivity to future climate change scenarios. Svalbard populations of Polar cod live in bottom waters with a temperature in between -1.5 and 3 °C, whereas long-term temperature acclimation in laboratory highlighted an optimal temperature between 3 and 6 °C (Kunz et al 2016; Leo et al 2017, 2020). A slight further increase in temperature to 8°C, however, caused increased mortality, a fall in the feed conversion efficiency, and an increase in the standard metabolic rate (Kunz et al 2016). Furthermore, Polar cod showed no lipid modification, hence no mitochondrial membrane adjustment (Leo et al. 2020), in line with an increase in proton leak, when facing high temperature (8 °C) conditions (Leo et al 2017). Therefore, 8 °C might be close to the long-term upper thermal tolerance limit of Polar cod, at least for the Svalbard population.

The role of increased pCO_2 in Polar cod response to climate change has not been thoroughly investigated, though when tested it showed little to no effects at least at the whole animal level (Kunz et al. 2016). Nevertheless, in a follow-up study on the same animals on the long-term exposure to warming and acidification conditions, Polar cod exhibited distinct modifications of cardiac enzyme capacities, with citrate synthase (CS) indicating a slight warm acclimation, and cytochrome *c* oxidase (COX) showing high sensitivity to both temperature and CO_2 treatments. This suggested an impact of CO_2 on mitochondrial functioning and warm acclimation in Polar cod (Leo et al. 2020).

3.7 Thesis hypothesis

This thesis followed the PhD projects of Kristina Kunz and Elettra Leo on the metabolism and performance of *B. saida* under future climate change conditions. This study aims to investigate the mitochondrial function of Polar cod specimens incubated for 4 months at four different temperatures (0, 3, 6, 8 °C) and two pCO_2, 390 ppm as present control level and 1170 ppm, a concentration projected for the year 2100 according to RCP 8.5 (IPCC, 2014). Although *B. saida* (as stated above) usually lives in much colder temperatures, it shows an optimal temperature range between 3 and 6 °C. Yet, long term acclimation to 8 °C revealed an inability of Polar cod to cope with slightly warmer temperatures (Kunz et al. 2016; Leo et al. 2017, 2020). For the present thesis, liver was chosen, as it represents the central hub for the metabolism of vertebrates and modifications in mitochondrial functions have already been demonstrated to be involved in the acclimation of ectothermal fish. Here, we aim at focussing on the molecular mechanisms involved.

Therefore, the first hypothesis of this thesis is: *The number of mitochondria significantly decreases as the temperature raises, with pCO_2 intensifying the temperature effect.* An important aspect of cold-adapted species is represented by the high density of mitochondria (Johnston et al. 1998; Pörtner et al. 2008), especially compared to temperate species (Johnston et al. 1998). Moreover, cold acclimation triggers an increase in mitochondrial volume density in ectotherms (O'Brien 2011). To differentiate between the possible mechanisms, increasing the number of mitochondria or to change the volume density of existing mitochondria, the relative number of mitochondrial DNA copies was determined by quantitative Realtime PCR of mitochondrial-encoded versus nuclear-encoded genes coding for key components of the mitochondrial energy metabolism.

The second hypothesis is: *The raising temperatures cause a significant decrease in expression of the genes involved in the oxidative phosphorylation* (*COX1, COX2, COX4, ND1, ND6, ATP6) and TCA cycle (CS), and high pCO_2 intensifies the temperature effect.* Several studies have already demonstrated transcriptional responses of mitochondrial genes upon thermal acclimation in temperate and cold-adapted fish (Lucassen et al. 2003, 2006; Windisch et al. 2011, 2014). Nevertheless, the response has never been related to the DNA copy number of the respective genes.

The third hypothesis is: *The enzyme function of and/or protein number of key mitochondrial components follow the responses at the mRNA level with high temperature and pCO_2 indicating a transcriptional regulation of mitochondrial*

functions. For this, maximum capacities of CS and COX were analysed together with quantification of the F_OF_1 ATP synthase by immunological methods.

The existing studies usually focussed on one or two aspects of the molecular cascade. Here, we aimed at aligning the responses at all three levels (DNA, mRNA, protein) to decipher the interplay between mitochondrial replication and transcriptional/translational regulation versus post-translational modifications of protein functions. This combined analysis will help to clarify the adaptational potential and the onset of mitochondrial dysfunction, which finally exerts their effects at the organismal level, under the threat of rising temperatures and ocean acidification.

4 Materials and methods

4.1 Experiment and data

This study aims to investigate responsiveness of mitochondrial functions in the Polar cod *Boreogadus saida* against future climate change scenarios of ocean warming and acidification. Therefore, the purpose is to quantify mitochondrial DNA, analyse the organelle's genes expression and the corresponding protein activity.

4.1.1 Animal collection and experimental design

The samples used in this study derive from specimen of *B. saida* captured in Kongsfjorden at the western coast of Svalbard in January 2013 by the R/V Helmer Hanssen, a research vessel belonging to the University of Tromsø (Norway). The fish were kept in the aquaria of the University of Tromsø and were transported in April of the same year to the aquaria of the Alfred Wegener Institute (AWI) in Bremerhaven (Germany). Here, after four weeks of acclimation to the laboratory conditions, the polar cod were incubated at a chosen set of temperatures (0, 3, 6, 8 °C) and CO_2 (390 and 1170 ppm), for a total of eight different temperature/CO_2 treatments. Each treatment consisted in 12 for a total of 96 Polar cod. Each specimen was measured (total length) and weighted in three crucial steps during the experiment: prior to the incubation, in the middle of the incubation period, and at the end of the experiment (after 130 days) (Kunz et al. 2016). The comprehensive study with several scientists involved was designed to access multiple factors from the molecular to the whole animal level. Therefore, 6 specimens per treatment were sampled directly at the end of the experiment (sampling round 1), whereas the other half of the specimens were used first for exercise studies and sampled later after full recovery (sampling round 2). These two sampling rounds were kept apart. Anyway, consecutive microarray analyses revealed no significant differences between both sampling rounds. Water chemistry specifics are shown in Table 4.1.

Table 4.1 **Water chemistry** for each treatment. Values are shown as mean ± SD throughout the total experimental period of 4 months. These and other water chemistry values are presented in Kunz et al. 2016.

Treatment (°C/ppm)	Salinity (psu)	pH_{tot}	PCO_2 (ppm)	Temperature (°C)
0/390	30.58 ± 0.98	8.08 ± 0.04	396.25 ± 37.70	0.90 ± 0.37
0/1170	30.70 ± 1.08	7.66 ± 0.05	1091.64 ± 131.67	0.61 ± 0.45
3/390	30.70 ± 1.01	8.05 ± 0.04	431.10 ± 40.41	3.15 ± 0.18
3/1170	30.74 ± 0.98	7.65 ± 0.05	1135.99 ± 147.10	3.06 ± 0.11
6/390	31.47 ± 0.53	8.03 ± 0.02	437.09 ± 21.60	5.63 ± 0.19
6/1170	31.49 ± 0.52	7.64 ± 0.03	1123.50 ± 86.23	5.57 ± 0.21
8/390	32.78 ± 0.82	8.05 ± 0.02	440.90 ± 29.10	8.16 ± 0.13
8/1170	32.71 ± 0.80	7.71 ± 0.05	1052.88 ± 103.87	8.11 ± 0.13

4.1.2 Samples

A total of 48 samples of liver tissue were selected for the current study (mostly from the first sampling round), 6 samples for each treatment combination: 0 °C/390 ppm, 0 °C/1170 ppm, 3 °C/390 ppm, 3 °C/1170 ppm, 6 °C/390 ppm, 6 °C/1170 ppm, 8 °C/390 ppm, 8 °C/1170 ppm. Each sample represents one different animal. To ensure that all data from the three extractions for DNA, RNA, and protein, respectively, can be correlated, in those cases, where not enough tissue was available, animals from sampling round 2 were taken. To do so, three sets of 48 samples, one for each analysis, were subsampled (according to the amount needed) on liquid nitrogen to avoid any thawing of the samples, weighted and stored at - 80 °C.

In Kunz et al. the length, the animal weight and the liver weight of each specimen were measured for the entire data set. In the present thesis, the respective data for hepatosomatic index (HSI) and the condition factor (K) from the used subset of animals are presented according to the following equations:

$$HSI = \frac{Liver\ weight}{Fish\ weight * 1000}\ 100 \qquad K = \frac{Fish\ weight * 100}{(total\ fish\ lenght)^3}$$

4.1.3 DNA extraction

A silica-based column extraction was chosen for DNA purification. Precisely, it was performed using the DNeasy Blood & Tissue Kit (Qiagen, Hilden, Germany), according to the manufacturer's instructions. Briefly, frozen liver samples of around

20 mg were lysed with proteinase K and incubated at 56 °C for 3 h in a thermomixer (Eppendorf, Hamburg, Germany). Following the incubation, RNase was added to the sample. The DNA, then bound to the silica column, was purified through consecutive washings and centrifugations. At the end the DNA was eluted twice with 50 µL of buffer AE.

The quality and amount of extracted DNA was assessed through NanoDrop 2000/2000c Spectrophotometer (ThermoFisher Scientific, Darmstadt, Germany) and the DNA samples were stored at -20 °C.

4.1.4 DNA extraction optimization

Prior to the above-mentioned DNA isolation, preliminary extractions were run on test samples of muscle and liver from *B. saida* to optimize the extraction protocol and the consecutive Realtime PCR. For this the best incubation period for the sample lysis, 3 h or overnight incubation, was determined and the effect of RNase treatment, which may remove copurified RNA from the DNA extract, was tested. Muscle samples were additionally chosen to have a better assessment of the different optimisation steps, given that muscle is a tissue with a high abundance of mitochondria.

The extracts obtained from the different procedures were checked through NanoDrop 2000/2000c Spectrophotometer (ThermoFisher Scientific, Darmstadt, Germany), agarose gel electrophoresis and Realtime PCR. The same samples were used for Primer optimization.

4.2 RNA expression

4.2.1 RNA extraction and cDNA synthesis

Total RNA was extracted using Qiazol lysis reagent and the Qiagen RNeasy kit (Qiagen, Hilden, Germany) according to the manufacturer's instructions. Briefly, frozen liver samples were added to 1 mL Qiazol and promptly homogenized at 6,000 rpm for 20 seconds at room temperature, using Precellys 24 (Bentin Instruments, Montigny-le-Bretonneux, France). After 5 minutes, 200 µL chloroform was added to the homogenate, mixed briefly, incubated for another 3 to 5 min and finally centrifuged at 12,000 g for 10 min (Microcentrifuge 24, Starlab, Hamburg, Germany). The upper phase was then transferred to a new tube, mixed with 600 µL of 70 % molecular-grade ethanol, from which 700 µL was applied to a RNeasy spin column. After centrifugation at 12,000 rpm for 30 seconds through a RNeasy spin column the flowthrough was discarded, the remaining mixture was

applied to the column and the centrifugation was repeated. The column was subsequently washed with 700 µL RW1 and twice with 500 µL RPE. The RNA bound to the spin column was finally eluted with two-times 50 µL of Tris-EDTA(TE)-buffer (10 mM Tris/HCl pH 8.0, 0.1 mM ethylenediaminetetraacetic acid (EDTA)). RNA samples quality and concentration was checked with a NanoDrop 2000/2000c Spectrophotometer and stored at - 80 °C.

To remove residual DNA impurities from the RNA extracts, a DNA digestion was performed using the TURBO DNA-*free* Kit (Invitrogen, ThermoFisher Scientific, Darmstadt, Germany). According to the manufacturer's instructions, 1.5 µg RNA of each sample was pre-diluted in 15 µL RNase free H_2O, and then 10 µL Mastermix was added to the diluted samples (Table 4.2), mixed thoroughly, and incubated for 30 min at 37 °C in a thermomixer.

Table 4.2 **Mastermix composition for DNase digestion.**

Mastermix components	1-fold Reaction
10-fold Buffer	2.5 µL
TURBO DNase	0.5 µL
Nuclease-free water	7.0 µL
Total:	10 µL

Subsequently, 2,5 µL of DNase inactivation reagent was added to the samples, incubated for 5 min at room temperature, and centrifugated at 13,200 rpm for 1.5 min (Eppendorf Centrifuge 5417 R, Eppendorf, Hamburg, Germany). The supernatant, which is DNA-free RNA, was then transferred to another tube and stored again at - 80 °C.

RNA samples were translated to DNA using the High-capacity cDNA reverse transcription kit from Applied Biosystems (ThermoFisher Scientific, Darmstadt, Germany) according to the manufacturer's instructions. Briefly, 0.4 µg of the DNA-free RNA samples were pre-diluted in 10 µL RNase-free water and the Reverse Transcriptase Mastermix was prepared (Table 4.3). 10 µL of final Mastermix was added to the sample and mixed. Reverse transcription was performed by means of an Eppendorf EP Gradient S Thermocycler (Eppendorf, Hamburg, Germany) following the user guide of the High-capacity cDNA reverse transcription kit (Applied Biosystems, ThermoFisher Scientific). Afterwards, the resulting samples were stored at - 20 °C.

Table 4.3 **Reverse Transcriptase (RT) Mastermix composition for cDNA synthesis.** The enzyme was added at last.

RT Mastermix components	1-fold Reaction
10-fold RT Buffer	2.0 µL
dNTP-Mix (25X; 100-mM)	0.8 µL
RT Random Primers (10fold)	2.0 µL
MultiScribe Reverse Transcriptase	1.0 µL
RNAse free H_2O	4.2 µL
Total:	10 µL

4.2.2 Quality control of RNA samples

The integrity of RNA extracts was determined on 12 chosen samples using an Agilent RNA 6000 Nano Kit and a 2100 Bioanalyzer (Agilent Technologies, Waldbronn, Germany), according to the manufacturer's instructions. Briefly, after decontaminating the electrodes, the RNA chip was positioned in the priming station and 9 µL gel-dye was pipetted in 2 wells and in the ladder well. Afterwards, 5 µL of the loading marker was pipetted in all 12 sample wells and an extra well, 1 µL of the RNA ladder in the ladder well and 1 µL of each sample in the 12 sample wells. Subsequently, the chip was run in the 2100 Bioanalyzer instrument within 5 min. The data were analysed using the building software of the instruments. RNA quality for consecutive Realtime PCR was considered as sufficient, if the RNA integrity number (RIN) was above 8.3.

4.3 Quantitative Realtime PCR

Primers of nuclear and mitochondrial genes were designed by means of the MacVector Software (Version 18.5.0, MacVector Inc.) and checked by the Primer Express Software (version 3.0, Applied Biosystems, ThermoFisher, Darmstadt, Germany). Primers were evaluated in terms of their potential to dimerise or loop (table 4.5). For the mitochondrially encoded genes, the published sequence by Breines et al. (2008; Accession number: NC_010121) was used and for the housekeeping gene β-Actin a published sequence from Genbank (Accession number: EU682944.1). All remaining genes were designed according to transcripts extracted from an unpublished Illumina-sequenced normalized transcriptomic cDNA library of *B. saida* liver (Windisch & Lucassen, unpublished), which was annotated against the SwissProt database (https://www.expasy.org/resources/uniprotkb-swiss-prot). All candidate transcripts

were checked manually in MacVector for sequencing artefacts and consistency of the annotation.

Prior to DNA and mRNA quantification, the chosen primers needed to be optimized to achieve highest efficiency in PCR reactions. To do so, DNA test samples were tested in a dilution series over 5 orders of magnitude (1, 0.1, 0.01 ng/µL, 1, 0.1 pg/µL of template) in TE-buffer. Forward- and reverse-primers were diluted in 100 µL with TE buffer to 5 µM aliquots, according to the concentrations certified by the manufacturer (Eurofins Genomics, Ebersberg, Germany). A 96 well-plate was used for the quantitative Realtime-PCR. Each reaction consisted of 2 µL of DNA template and 18 µL of Realtime master mix, composed of 300 nM forward and reverse primer each, nuclease-free H_2O, and SYBR Green PCR Master Mix (Applied Biosystems, ThermoFisher Scientific, Darmstadt, Germany). A duplicate control for each primer was obtained by substituting the template with 2 µL of nuclease-free H_2O instead of the template (= no template control). Primer optimization was done in triplicates for each dilution step using a Viia7 RT-PCR system (Applied Biosystems, ThermoFisher Scientific, Darmstadt, Germany). Table 4.4 shows the PCR program used.

Table 4.4. **Setup of the quantitative Realtime PCR conducted by Viia7.**

Step/Cycle	Period	Temperature
Step 1	2 min	50 °C
1 cycle	10 min	95 °C
Step 2	15 s	95 °C
40 cycles	1 min	60 °C
Step 3	15 s	95 °C
Melt Curve	1 min	60 °C
Continuous	15 s	95 °C

The specificity of the amplification was checked by melt curve analysis. Only those reactions with one reliable peak in the melting curve were used for consecutive determination of the critical threshold (Ct) values. The efficiency (*E* in the equation) of the primer pairs was determined through the construction of a calibration curve, where the $\log_{10}$ of template concentration was plotted against the Ct value. Efficiencies ranging from 1.8 to 2.1 were accepted (Table 4.5).

$$E = 10^{-1/Slope}$$

DNA and mRNA quantification was conducted through duplicates, using 2 µL of templates, containing 2 ng of nucleic acids, and 18 µL of Realtime master mix. The software “QuantStudio Real-Time PCR Software v1.2” (Applied Biosystems,

ThermoFisher Scientific, Darmstadt, Germany) was used to calculate the Ct values from the amplification curves. Gene expression differences between treatments were analysed using the comparative -$\Delta\Delta C_T$- method with treatment 0 °C; 390 ppm as control (Livak & Schmittgen 2001). The data were normalized with respect to the housekeeping genes Ubiquitin and β-Actin. Data are presented as log2fold change (= (-ΔΔCt)) to ensure an equal representation of up and down regulation.

Table 4.5 **Primer data for quantitative Realtime PCR.**

Gene Location	Protein/gene	Oligo name	Sequence (5'→3')	Efficiency	Accession number
Nuclear DNA	**Cytochrome *c* oxidase subunit 4 (COX4)**	Bs-COX4_FP2 Bs-COX4_RP2	GGCCACGCTCTCCAATGA GCAAAGCTCTGTTTGAAGCTGAT	1.93	Unpublished
	Citrate synthase (CS)	Bs-CS_FP2 Bs-CS_RP2	AGCAGGGCAAGGCAAAGA GCAGGAGCACCCCACTGT	1.85	Unpublished
	β-Actin (βAct)	Bs_bAct_FP7 Bs_bAct_RP7	CCTTCCTCGGTATGGAGTCTTG CGCACTTCATGATGCTGTTGT	1.97	EU682944.1
	Ubiquitin (Ubi)	Bs_Ubi_FP1 Bs_Ubi_RP1	AATGCTTGCCCAGAAGTACAACT AGGCGGGCATAGCACTTG	1.92	Unpublished
Mitochondrial DNA	**Cytochrome *c* oxidase subunit 1 (COX1)**	Bs_COX1_FP21 Bs_COX1_RP21	TCTGCATGGAGGCTCAATTA CCCCAACTGTAAAGAGGAAAAT	1.97	NC_010121
	Cytochrome *c* oxidase subunit 2 (COX2)	Bs_COX2_FP23 Bs_COX2_RP23	GACTTAGCCCCTGGTCAATT TGGGAGATTCAACTGGAACA	1.92	NC_010121

Gene Location	Protein/Gene	Oligo Name	Sequence (5'→ 3')	Efficiency	Accession number
Mitochondrial DNA	**NADH-ubiquinone oxidoreductase chain 1 (ND1)**	Bs_ND1_FP4 Bs_ND1_RP4	CTTTGTACTCGCCCTCTCAA GCTCAGCCAGAACCTAGAAT	1.91	NC_010121
	NADH-ubiquinone oxidoreductase chain 1 (ND1)	Bs_ND1_FP5 Bs_ND1_RP5	ACGGACTCCTTCAACCAATT AGGGCGAATGGGTTCTTTAA	1.93	NC_010121
	NADH-ubiquinone oxidoreductase chain 6 (ND6)	Bs_ND6_FP36 Bs_ND6_RP36	GGGTCTGTGTTAGGTTATTT CATATCACCCTCCCCAAAAT	2.00	NC_010121
	ATP synthase F_o subunit 6 (ATP6)	Bs_ATP6_FP20 Bs_ATP6_RP20	CGCCTACTTCACGATGATTAA AGTAAAGCGGGCGATAAAT	2.00	NC_010121

4.4 Enzymatic capacities of mitochondrial key enzymes

4.4.1 Buffers

A total of three buffers was used for protein extraction and analysis of maximum capacities of the mitochondrial key enzymes cytochrome *c* oxidase (COX) and citrate synthase (CS). The extraction buffer (EB1) for both enzymes consisted of 20 mM Tris HCl with a pH of 8.0. COX activity was measured in a COX assay buffer containing 20 mM Tris HCl buffer and 0.05 % Tween 20 at a pH of 7.9. The CS assay buffer consisted of 75 mM Tris HCl buffer with a pH of 8.0. As Tris buffer respond quite reasonable to temperature, all pH were adjusted at a temperature of around 0 °C with calibration buffers acclimated to the same temperature, close natural habitat temperature of the fish and to the temperatures used in the final enzyme assays.

4.4.2 Optimization of enzyme extraction

Enzyme extractions required a thorough optimization for maximum recovery of functional enzyme and reproducible quantity, especially in liver containing high amounts of lipids in gadid fish, which may cause extensive scattering during the spectrophotometrical measurements. Liver test samples were used for the optimization and three different lysis methods were tested.

1. Lysis through homogenization at 5000 rpm and 4 °C, once for 20 seconds with a Precellys 24 Micro Mill System (Bentin Instruments).
2. Hand homogenization (2 mL glass-glass homogenizer) combined with additional homogenization using a T-25 digital Ultra-Turrax (IKA, Staufen Germany)
3. Hand homogenization (2 mL glass-glass homogenizer).

In each case the frozen tissue was directly transferred into the respective vessel and homogenized instantaneously. Hand homogenization was performed until no tissue debris were visible anymore and was continued for another minute. The Ultra Turrax was used at 10,000 rpm for 10 s interrupted by intermediate cooling in ice water for 30 s. Afterwards, the samples were tested for maximum enzyme activity (COX and CS: see 4.4.4) to compare the different methods. Further spectrophotometric analyses were run to determine whether the removal of lipids forming an upper phase after the centrifugation was necessary to improve the measurements.

4.4.3 Final enzyme isolation

Hand homogenization alone was chosen as preferential protein extraction method. Briefly, 48 liver samples of around 100 mg each were hand-homogenized in 10 volumes of ice-cold extraction buffer EB1. The lysed samples were centrifuged at 1,000 g and 0-4 °C for 10 min (Eppendorf Centrifuge 5417 R) to remove cell debris. Afterwards, before transferring the crude extract (supernatant) to another tube, the lipids stratified on top of the samples were carefully removed by pipetting. An aliquot of 50 µL crude extract was directly removed and stored at - 20 °C for further analysis (see 4.4.6 and 4.4.7) and the rest of the extract was immediately used for the spectrophotometric analysis.

4.4.4 Spectrophotometric determination of maximum enzyme activities

The maximum activity of CS and COX was analysed in 48 protein samples. Prior to the analysis, cytochrome *c* was reduced using a PD-10 desalting column (Amersham Biosciences, Uppsala, Sweden), according to the manufacturer's instructions. Briefly, after removing the storage buffer and washing with excess H_2O, the column was equilibrated with 25 mL of extraction buffer EB1, which was degassed with nitrogen for about 30 min. 100 mg cytochrome *c* was dissolved in 2.5 mL EB1 and then reduced with a small amount of sodium dithionite and directly applied to the column. The flow-through (2.5 mL) was discarded and the reduced cytochrome *c* was eluted with 3.5 mL degassed EB1. Afterwards, cytochrome *c* was aliquoted in brown HPLC vials and stored at - 20 °C.

The analysis of CS and COX maximum activity was performed on an Analytik Jena Specord S 600 (Analytik Jena, Jena, Germany) with a cooling device and the slope ($\Delta E/\Delta t$) was determined with the software WinASPECT (Analytik Jena, Jena, Germany). For both enzymes (CS and COX) each sample was run in duplicates of which one was the double amount of the other. Before, different amounts of extracts were tested to reach sufficient speed and to make sure that the respective extract and no other component of the assay limit the reaction rate. All assays were performed at two temperatures: 0 °C as it represents the control temperature for the species and 10 °C to assess the Q_{10} effect of the enzymes.

CS activity was determined according to Sidell et al. (1987) from the increase in absorbance at 412 nm, given by the transfer of the sulfhydryl group from coenzyme A (CoA) to 5,5′-dithiobis-(2-nitrobenzoic acid) (DTNB). The extinction coefficient used was $\varepsilon_{412} = 13.61\ mol^{-1}\ cm^{-1}$. The reaction mixture consisted of 75 mM Tris/HCl pH 8.0, 0.25 mM DTNB, 0.5 mM oxaloacetate, 0.4 mM Acetyl-

CoA. Briefly, in a volume of 1 mL, 15 and 30 µL of sample, respectively, was set up with all component but oxaloacetate and equilibrated in the photometer for 5 min. The reaction was started with oxaloacetate after the pre-run reached a plateau and followed for about 10 min.

COX activity was determined according to a modified protocol after Moyes et al. (1997) from the decrease in extinction at 550 nm, given by the oxidation of reduced cytochrome *c*, using an extinction coefficient of $\varepsilon_{550} = 19.1\ mol^{-1}\ cm^{-1}$. The reaction mixture (1 mL) consisted of 20 mM Tris/HCl pH 8.0, 0.05 % (v/v) Tween 20 and 0.057 mM reduced cytochrome c_{red}. Briefly, 965 (955) µL pre-cooled assay buffer was mixed with 25 µL reduced cytochrome *c* and equilibrated for 5 min in the spectrophotometer. After the firsts few cycles of reading 10 (20) µL of sample was added and mixed. The reaction was followed for the following 5 min.

4.4.5 Enzyme activity and temperature coefficient

COX and CS enzyme activities were related to the fresh weight and obtained from the following equation:

$$U = \frac{\Delta E}{\varepsilon} \frac{V_{tot}}{V_S} \frac{V_B}{fwt}\ 60\ [\mu mol * h^{-1} * g^{-1}]$$

Where: ΔE is the difference between the maximal slope in the linear range after the start of the reaction and the prerun, ε is the extinction coefficient, V_{tot} is the total volume in the cuvette (always 1 mL), V_S is the volume of the sample, V_B is the volume of the extraction buffer used for protein isolation, *fwt* is the fresh weight of the sample used. The enzymes are presented as the natural logarithm of fresh weight related activities for better comparison with the RNA and DNA data.

The temperature coefficient Q_{10} was calculated from the natural logarithm of the enzymes activity. The equation used is as follows:

$$Q_{10} = e^{(A_{10}-A_0)/(T_{10}-T_0)\ 10}$$

Where A_{10} and A_0 represents the natural logarithm of enzyme activity at 10 °C and 0 °C, respectively; T_{10} and T_0 represents the assay temperatures, respectively.

4.4.6 Determination of protein concentrations via Bradford

Protein quantification was carried out according to Bradford (1976), which is based on the change in absorption of the dye *Coomassie Brilliant Blue G-250* upon binding to proteins. Briefly, each sample was diluted 10fold with extraction buffer

EB1. Protein determination was performed in a microplate in triplicates with 10 µL of each sample and 250 µL of Bradford-Solution (PanReac AppliChem, Darmstadt, Germany). A duplicate control for each plate was obtained by substituting 10 µL of the sample with H_2O. For the calibration curve, 5 standards were prepared from a bovine serum albumin (BSA) stock solution (1 mg/mL) as shown in Table 4.6.

Table 4.6. **BSA standard series.**

	BSA-Stock [µL]	H2O [µL]	BSA [µg/well]
Standard 1	20	80	2
Standard 2	40	60	4
Standard 3	60	40	6
Standard 4	80	20	8
Standard 5	100	0	10

After 10 min of incubation at room temperature, the optical density at 595 nm was recorded by means of an BioTeck PowerWave HT Microplate Reader (Agilent Technologies, Waldbronn, Germany) and the data were analysed by the BioTek Gen5 Software for Imaging & Microscopy (Agilent Technologies).

4.4.7 Immunological detection of proteins

Immunological detection (“Western blotting") and related quantification were performed for the mitochondrial F_OF_1 ATP synthase. First, sodium dodecyl sulphate polyacrylamide gel electrophoresis (SDS-PAGE) was conducted according to Laemmli (1970) to separate the protein of the crude extracts by molecular size. Briefly, a 10 % separation gel was prepared with separation gel buffer (375 mM Tris/HCl pH 8.8, 0.1 % SDS), acrylamide solution (acrylamide/bis acrylamide 37.5:1), 1 mg/mL ammonium persulfate (APS) and 0.1 % tetramethylethylenediamine (TEMED). The 4 % stacking gel was prepared from stacking gel buffer (0.125 M Tris/HCl pH 6.8 and 0.1 % SDS), acrylamide solution, 1 mg/mL APS and 0.05 % TEMED. TEMED was added at the end to start the polymerisation. The SDS-PAGE was performed in a Mini Protean III System (Biorad, Munich, Germany). The homogenised samples were denatured by 2:1 dilution with 3x-SDS loading buffer (62.5 mM Tris/HCl pH 6.8, 2 % SDS, 0.005 % bromphenolblue, 10 % glycerine, 5 % mercaptoethanol).

Five random samples were mixed for the standard curve dilution series. The composition of these standards for the SDS-PAGE are shown in Table 4.7. As a modification of existing protocols, the loading amount of protein per lane was

balanced by adding BSA as unrelated protein to each sample. All protein samples were separated in electrophoresis buffer (25 mM Tris, 192 mM glycine, 0.1 % (w/v) SDS) by SDS-PAGE at 200 V for approximately 60 min. For determination of the molecular weight, 6 µL prestained SDS-PAGE standard (Biorad) was running in parallel.

Table 4.7 **Dilution series of protein extracts for Western blotting**

a) Standard curve obtained by mixing 5 random samples.

N°	Crude extract for each lane (µL)	Estimated Protein for each lane *) (µg)	Crude Extract (from five random samples) (µL)	Bovine serum albumin (BSA) **) (µL)	SDS Mix (µL)	Volume per lane (µL)
Marker						6
S1	0.50	1.50	1.50	58.50	30	15
S2	1.00	6.00	6.00	54.00	30	15
S3	2.00	12.00	12.00	48.00	30	15
S4	4.00	24.00	24.00	36.00	30	15
S5	8.00	48.00	48.00	12.00	30	15

b) All samples: Dilution according to S3.

	Crude extract for each lane (µL)	Estimated Protein for each lane (µg)	Crude Extract (µL)	BSA (µL)	SDS Mix (µL)	Volume per Lane (µL)
Samples	2.0	12.0	6.00	24.00	15	15

***) For estimation of the protein content per lane an average content of 5 mg/mL protein was assumed for the crude extract, **) BSA stock solution: 1 mg/mL.**

For Western blotting the TransBlot Cell XY (Biorad) was used according to the manufacturer's instructions. Briefly, blotting was performed in transfer buffer pH 9.5-9.9 (10 mM $NaHCO_3$, 3 mM Na_2CO_3, 20 % methanol, 0.025 % SDS) on PVDF membranes (first wetted in 100 % methanol, then equilibrated in transfer buffer). After the SDS-PAGE, the gels were equilibrated in transfer buffer, and subsequently the sandwich consisting of membrane, gel, blotting paper and fiber pads was assembled in the blot apparatus. The electro transfer took place for 3 hours at 35 V and 4 °C. After disassembling the sandwich, the PVDF membranes were incubated for 1 h in blocking buffer (5 % skimmed milk powder in 1xTBS-T

washing buffer (50 mM Tris/HCl pH 7.4, 0.9 % NaCl, 0.1 % Tween 20)) at room temperature to saturate non-specific binding of proteins to the membrane. 1 µL of the bovine protein-specific antibody for the F_OF_1 ATP Synthase (Raised against complex V: Anti-ATP5A, Abcam Antibodies, Cambridge, UK) was diluted in 5 mL of blocking buffer. Lastly, the membranes were placed in a foil bag with the diluted antibody and incubated on a shaker overnight at 4 °C. Subsequently, the membranes were washed (three times in TBS-T) and incubated with Horseradish Peroxidase-conjugated Goat-Anti-Mouse IgG Antibody (1:20,000 in 10 mL blocking buffer) for 1 h at room temperature, and washed again three times in TBS-T.

4.4.8 Detection

The detection of the bound antibody was carried out by means of a CCD-camera (LAS-1000, Fujifilm, Düsseldorf, Germany) using the ECL-System (GE Healthcare LifeSciences, AmershamBiosciences, Freiburg, Germany). The AIDA Image Analyzer software (Raytest, Straubenhardt, Germany, AIDA BioPackage) was used to calculate the intensity of the different protein bands.

4.4.9 Optimization of quantitative Western blotting

BSA (Bovine Serum Albumin) was tested in the SDS-PAGE to equalize the amount of protein and to get a good distribution of the protein sample especially in those lanes with small extract volume. By using this dilution step with unrelated protein, the same volume could be applied to each lane.

Dilution series were used on each final Western blots where the 48 samples were applied randomly. Quantification of the samples were done according to the respective gel. Two different calibration curves were obtained for each gel, a linear and a polynomial, to be used for protein quantification. Indeed, linear regression better represented the lower part of the standard series, whereas the polynomial fit better displayed the upper part. For each calibration curve a breakpoint was defined so that samples were quantified according to the calibration curve, to which range the signal belonged to.

4.5 Statistical analysis

Statistical analyses were conducted with SigmaPlot 12.5 (Systat Software, Erkrath, Germany). All graphs were designed with SigmaPlot 12.5, as well. All values are given as mean with standard error of the mean. DNA and mRNA expression were tested for both using two-way ANOVA with temperature and pCO_2 as factors, followed by Student-Newman-Keuls pairwise comparison tests ($\alpha = 0.05$).

Additionally, gene expression for both DNA and mRNA was tested with linear regression as well (separate for both pCO_2 levels). Hepatosomatic Index (HSI), condition factor, normalized DNA and RNA content, along with the treatments, were tested with two-way ANOVA and linear regression. Protein quantity, F_OF_1 ATP synthase protein expression, CS and COX activity along with treatments, were tested with two-way ANOVA and linear regression. Normal distribution of data was checked with Shapiro-Wilk test ($p > 0.05$) and homogeneity of variance with Levenne's test ($\alpha = 0.05$). Technical outliers were identified by Nalimov's test and excluded ($\alpha = 0.01$).

5 Results

5.1 Hepatosomatic index and condition factor

Since the used samples in the present thesis represent only a subset of the former study by Kunz et al. (2016), HSI and whole animal parameters are presented here for the used animals, as they may influence the mitochondrial functioning in liver. Two-way ANOVA showed no effect of both temperature and pCO_2 on HSI, but a significant effect of temperature on condition factor ($p < 0.001$) (Figure 5.1). Since the factor temperature has a directional effect, linear regression was applied alternatively, demonstrating a significant effect of temperature ($p = 0.002$) on HSI at control pCO_2 levels, which increases with higher temperature. With linear regression, increasing temperature had a strong negative effect on the condition factor at control pCO_2 ($p < 0.001$) and moderate effect at high pCO_2 level ($p = 0.038$).

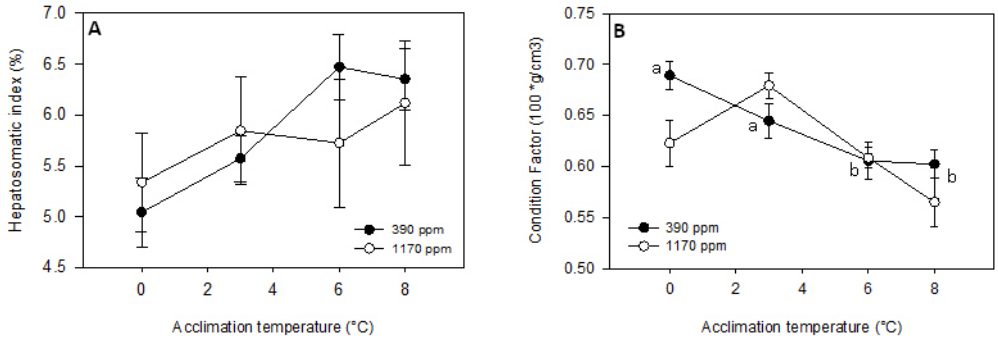

Figure 5.1 **Hepatosomatic Index and Condition factor of *B. saida*.** HSI (**A**) and condition factor (**B**) were calculated from the fish weight and length, and from liver weight. (390 ppm: filled circles; 1170 ppm: open circles). Significantly different groups are characterized by different letters. Error bars display standard error.

5.2 DNA quantification

DNA expression levels were calculated from DNA concentration in ng/µg and presented as log2-fold-change relative to the endogenous control genes *ubi* and *βact*. For clarification, values of 0 represent a stable expression, while a log2fold change of + 1 depicts a 2fold upregulation.

5.2.1 DNA extraction and content

For reliable determination of the mitochondrial copy number, both DNA extraction methods and Realtime qPCR conditions including primer validation, had to be optimized in concert. Realtime qPCR results of test samples delineated a preferential method for DNA extraction. C_T values of test samples, in fact, presented no significant differences between 3 h and overnight incubated samples (both with an average of around 19). Oppositely, C_T values of samples treated with RNase where much lower than C_T values of samples not treated with RNase (average of 17 against 20, respectively) indicating higher amounts of template in the Realtime qPCR on RNase treated samples (Figure 5.2). Thus, relative concentration of DNA increases if RNA impurities have been removed. This effect was stronger in the 3 h digested samples, as more RNA might have been already digested upon overnight DNA extraction. Although the total DNA yield after RNase treatment was reduced significantly, this step was introduced into the final extraction protocol to obtain more reliable data for the DNA content.

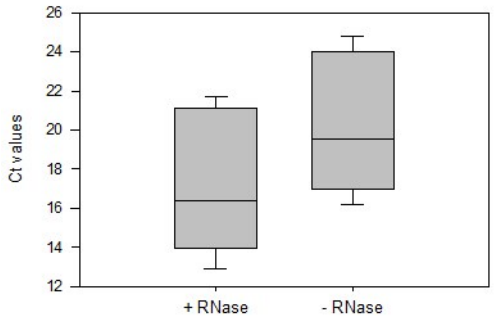

Figure 5.2 **DNA optimization.** Comparison between C_T values of DNA extracted with RNase and without RNase.

The DNA content in the liver per mg fresh weight ranged from 0.045 to 0.718 µg/mg fresh weight. No temperature and pCO_2 effect were found on DNA content by means of Two-way ANOVA or linear regression (Figure 5.3).

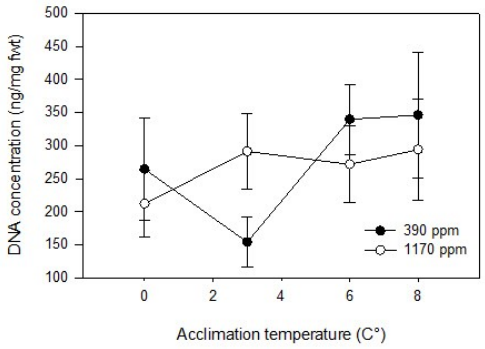

Figure 5.3 **Total DNA content in liver samples of *B. saida*.** The DNA concentration was obtained from the NanoDrop 2000/2000c Spectrophotometer analysis. The concentration is expressed as ng/mg fresh weight (390 ppm: filled circles; 1170 ppm: open circles). A significance level of $\alpha = 0.05$ was chosen for Two-way ANOVA. Error bars display standard error.

5.2.2 Quantification of nuclear genes

The aim of the present study was to determine the copy number of the mitochondrial genome relative to the nuclear chromosomal DNA. For this normalization, four nuclear genes have been included into the study, and tested for the stable expression. In general, *cox4*, *ubi*, *βact*, and *cs* were always expressed at constant levels and were not affected by temperature, nor by pCO_2 treatments (Figure 5.4). Since *cox4* and *cs* represent both nuclear genes that are essential for mitochondrial function, the mean of *ubi* and *βact* was finally used as endogenous control in the calculation according to the -$\Delta\Delta C_T$- method.

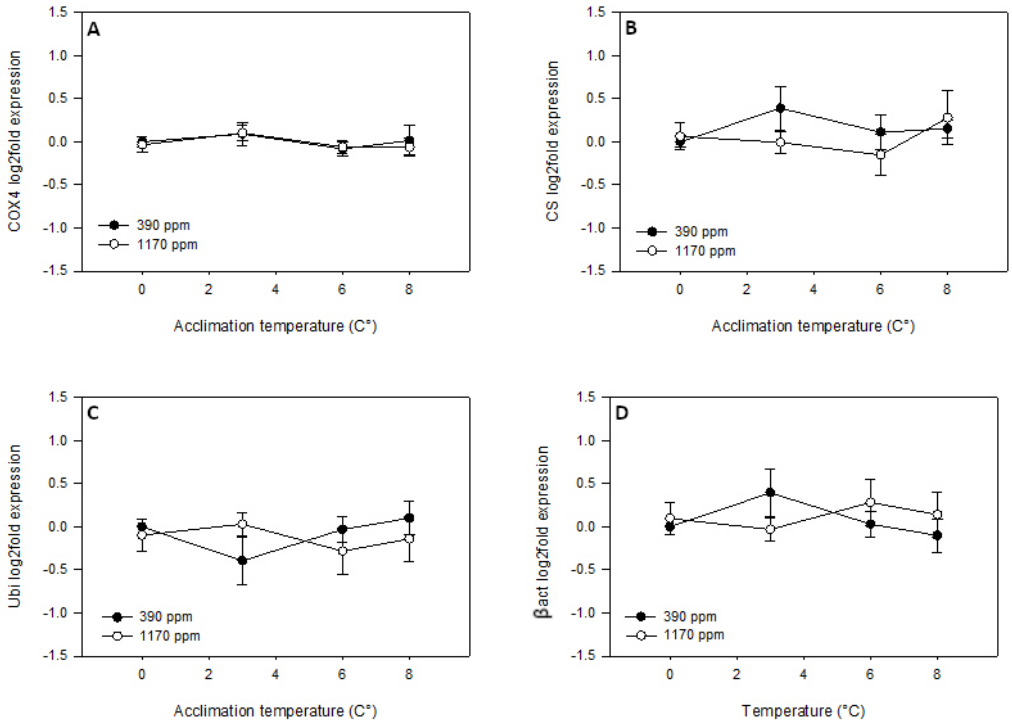

Figure 5.4 **DNA log2fold expression of nuclear genes of *B. saida*** after 130 days of acclimation to control conditions (0 °C and 390 ppm) and to a combination of three elevated temperatures (3, 6, 8 °C) with control (390 ppm) and high pCO_2 (1170 ppm). The data were normalized to the mean Ct values of Ubi and βAct as endogenous control. 0 °C, 390 ppm pCO_2 was normalized to 0 (390 ppm: filled circles; 1170 ppm: open circles). A significant level of $\alpha = 0.05$ was chosen for Two-way ANOVA. Error bars display standard error.

5.2.3 Quantification of mitochondrial encoded genes

Mitochondrial encoded gene expression exhibited much higher factorial variance than the nuclear-encoded genes studied here, with only few significant effects (Figure 5.5). Generally, two groups of response could be detected. *cox1* and *cox2* grouped together showing a different pattern than *nd1* (ND1_4, ND1_5) and *atp6*. *nd6*, the only gene encoded on the opposite strand of the mitochondrial genome followed the pattern of the second group for the control pCO_2 but differed with respect to high pCO_2. At least *nd1* showed a moderate effect caused by the interaction of temperature and pCO_2. Whereas the expression remains constant for all temperatures under high pCO_2 level, it dropped down significantly by a factor of about two (log2fold change = - 1) for both primers ND1_4 ($p = 0.035$) and ND1_5 ($p = 0.044$) at 8 °C under control pCO_2. Linear regression confirmed the downregulation of *nd1* caused by the exposure to a high pCO_2 ($p = 0.031$ for ND1_4; $p = 0.043$ for ND1_5) (Figure 5.5, **C**, **D**).

To level the noise of single genes along the Realtime qPCR quantification the mean of ND1_4, ND1_5 and ATP6 were analysed as representative pattern for the mitochondrial-encoded genes. Again, a pCO_2 effect became visible at 8 °C with 2fold lower expression under control pCO_2 (Two-way ANOVA $p = 0.034$; slope of linear regression $p = 0.032$) (Figure 5.5, **G**).

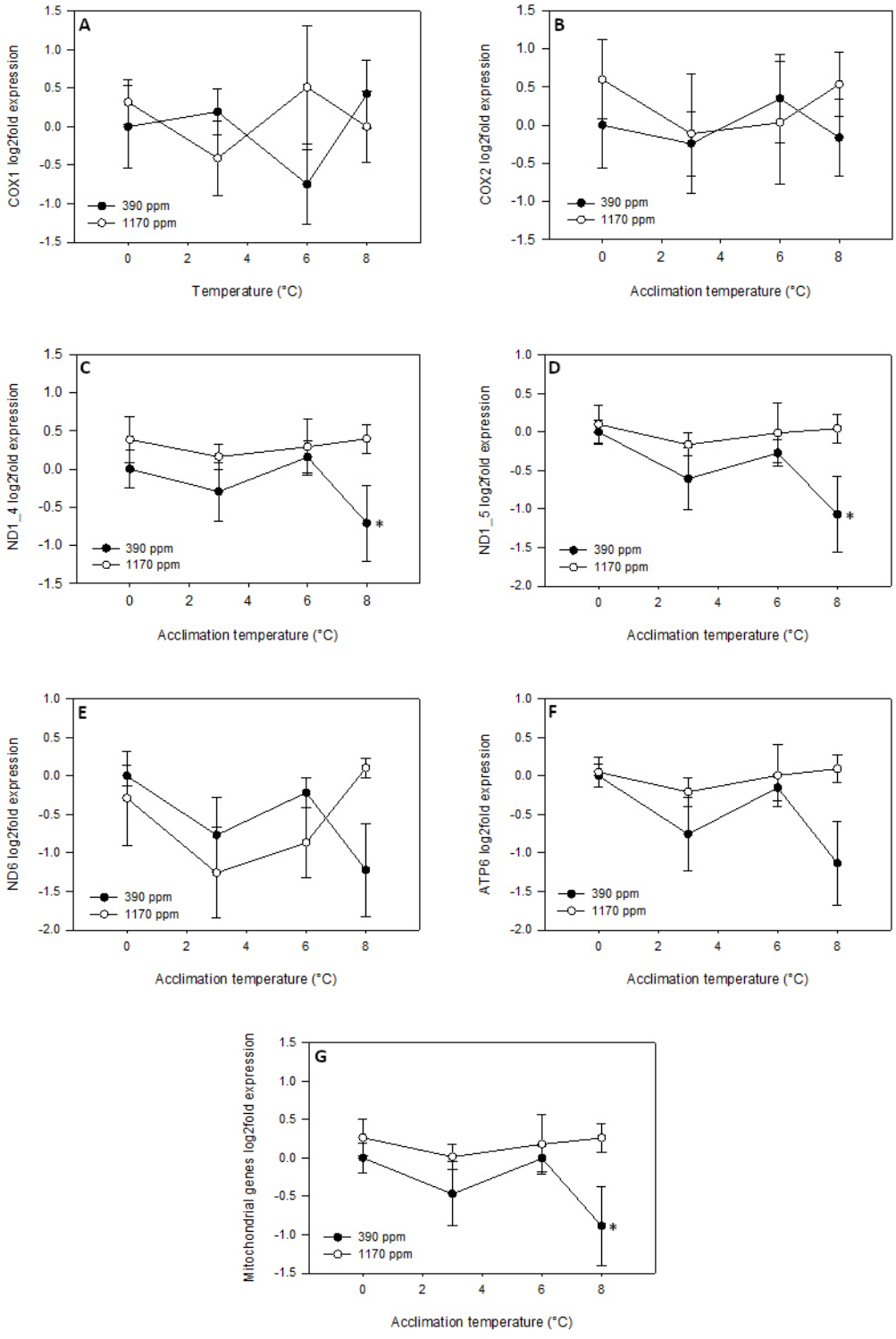
A
COX1 log2fold expression
Temperature (°C)
B
COX2 log2fold expression
Acclimation temperature (°C)
C
ND1_4 log2fold expression
Acclimation temperature (°C)
D
ND1_5 log2fold expression
Acclimation temperature (°C)
E
ND6 log2fold expression
Acclimation temperature (°C)
F
ATP6 log2fold expression
Acclimation temperature (°C)
G
Mitochondrial genes log2fold expression
Acclimation temperature (°C)
390 ppm
1170 ppm
*

Figure 5.5 **DNA log2fold expression of mitochondrial genes** of *B. saida* after 130 days of acclimation to control conditions (0 °C and 390 ppm) and to a combination of three elevated temperatures (3, 6, 8 °C) with control (390 ppm) and high pCO_2 (1170 ppm). The data were normalized to mean Ct values of Ubi and βAct. 0 °C, 390 ppm pCO_2 was normalized to 0 ANOVA (390 ppm: filled circles; 1170 ppm: open circles). A significant level of $\alpha = 0.05$ was chosen for Two-way ANOVA. * represents an effect of pCO_2. The error bars display standard error.

5.3 mRNA expression

mRNA expression levels were calculated per µg RNA and presented as log2fold-change relative to the endogenous control genes *ubi* and *βact* in the same way as for the DNA quantification to allow meaningful comparisons of both molecular markers. For clarification, values of 0 represent a stable expression, while a log2 fold change of +1 depicts a 2fold upregulation.

5.3.1 RNA quality and content

RNA content in the liver per mg fresh weight was in the range of 0.336 to 5.452 µg/mg and varied reasonable between animals. Nevertheless, RNA concentration significantly decreased with increasing temperatures ($p < 0.001$) (Figure 5.6). Particularly, sharp decrease in RNA content of almost a factor 3 was registered between 0 and 8 °C ($p < 0.001$) without an effect of pCO_2. Linear regression confirmed the temperature effect on the decrease of RNA concentration ($p < 0.001$).

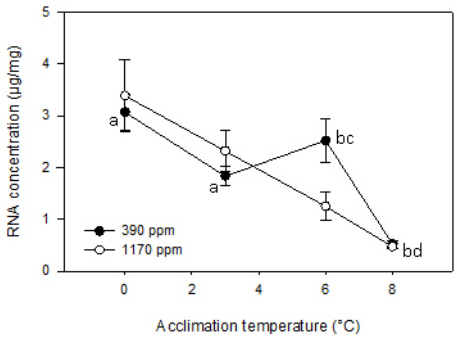

Figure 5.6 **Total RNA concentration in liver samples of *B. saida*.** The RNA concentration was obtained from the NanoDrop 2000/2000c Spectrophotometer analysis. The concentration is expressed as µg/mg and the error bars display standard error (390 ppm: filled circles; 1170 ppm: open circles). A significant level of $\alpha = 0.05$ was chosen for Two-way ANOVA. Significantly different groups are characterized by different letters, dots signed with *bc* and *bd* represent groups that are significantly different from the others and between themselves.

5.3.2 Expression of nuclear genes

cox4 was significantly downregulated almost 2fold with rising temperatures ($p = 0.017$) (Figure 5.7, **A**). Neither pCO_2 nor combined temperature-pCO_2 increase influenced *cox4* expression. Linear regression showed a significant downregulation of *cox4* caused by temperature treatment ($p = 0.004$), which did not differ with respect to pCO_2.

A slight downregulation of *cs* was found to be related to rising temperatures ($p = 0.033$), in particular between 3 and 8 °C ($p = 0.028$) (Figure 5.7, **B**). CO_2, as well as CO_2 combination with temperature, had no general effect on *cs*. Linear regression showed a downregulation of *cs* as an effect of temperature ($p = 0.010$).

In comparison *ubi* and *βact* expression was much more stable, and consequently a good choice to be taken as endogenous control. Neither temperature nor CO_2 treatments were found to have a significant effect on the expression of both genes (Figure 5.7, **C**, **D**).

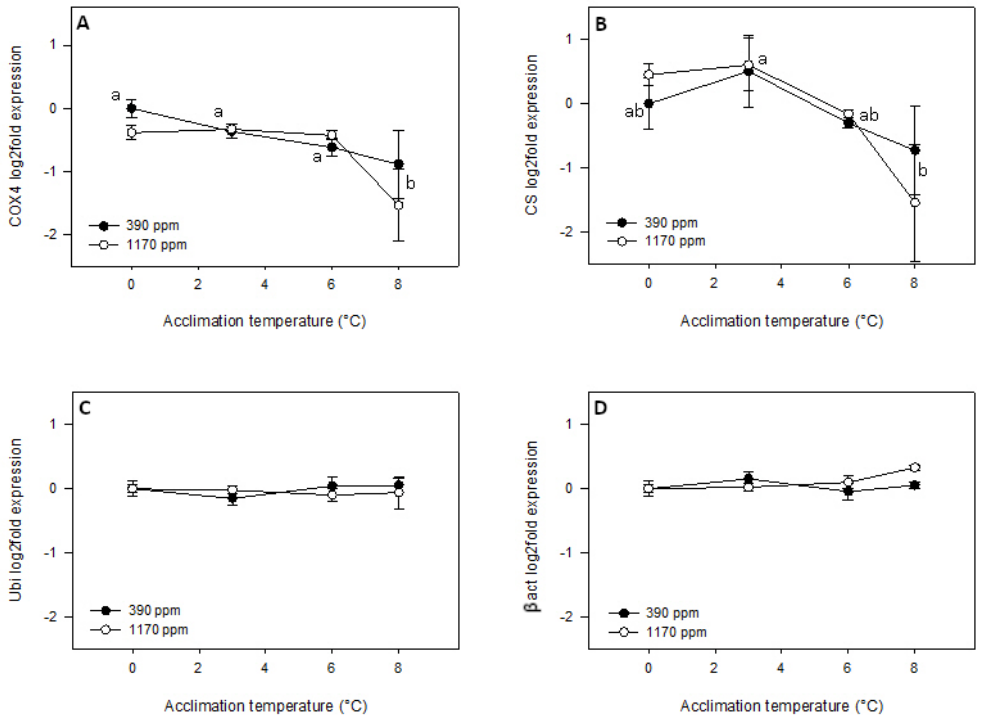

Figure 5.7 **mRNA log2fold expression of nuclear genes** of *B. saida* after 130 days of acclimation to control conditions (0 °C and 390 ppm) and to a combination of three elevated temperatures (3, 6, 8 °C) with control (390 ppm) and high pCO_2 (1170 ppm). The data were normalized to mean Ct values of Ubi and βAct. 0 °C, 390 ppm pCO_2 was normalized to 0 (390 ppm: filled circles; 1170 ppm: open circles). A significant level of $\alpha = 0.05$ was chosen for Two-way ANOVA. Significantly different groups are characterized by different letters, dots signed with *ab* represents intermediate groups, that are not significantly different from the others. The error bars display standard error.

5.3.3 Expression of mitochondrial-encoded genes

No significant change in expression was registered with COX1, COX2 and ND1_4 following the raise in temperature and pCO_2. ND1_5 was not affected when analysed by two-factor ANOVA, whereas a significant declining slope due to temperature could be detected according to linear regression for the high pCO_2 group ($p = 0.043$) (Figure 5.8).

nd6 was found downregulated by about a factor 2 due to temperature ($p = 0.016$), but no pCO_2 effect (Figure 5.8, **E**). This could be verified by linear regression ($p = 0.003$). A similar pattern was obtained for *atp6*, which steeply decreases with increasing temperature ($p < 0.001$). No effect of pCO_2 on *atp6* was registered. A strong downregulation by temperature on *atp6* was observed also with linear regression ($p < 0.001$) (Figure 5.8, **F**).

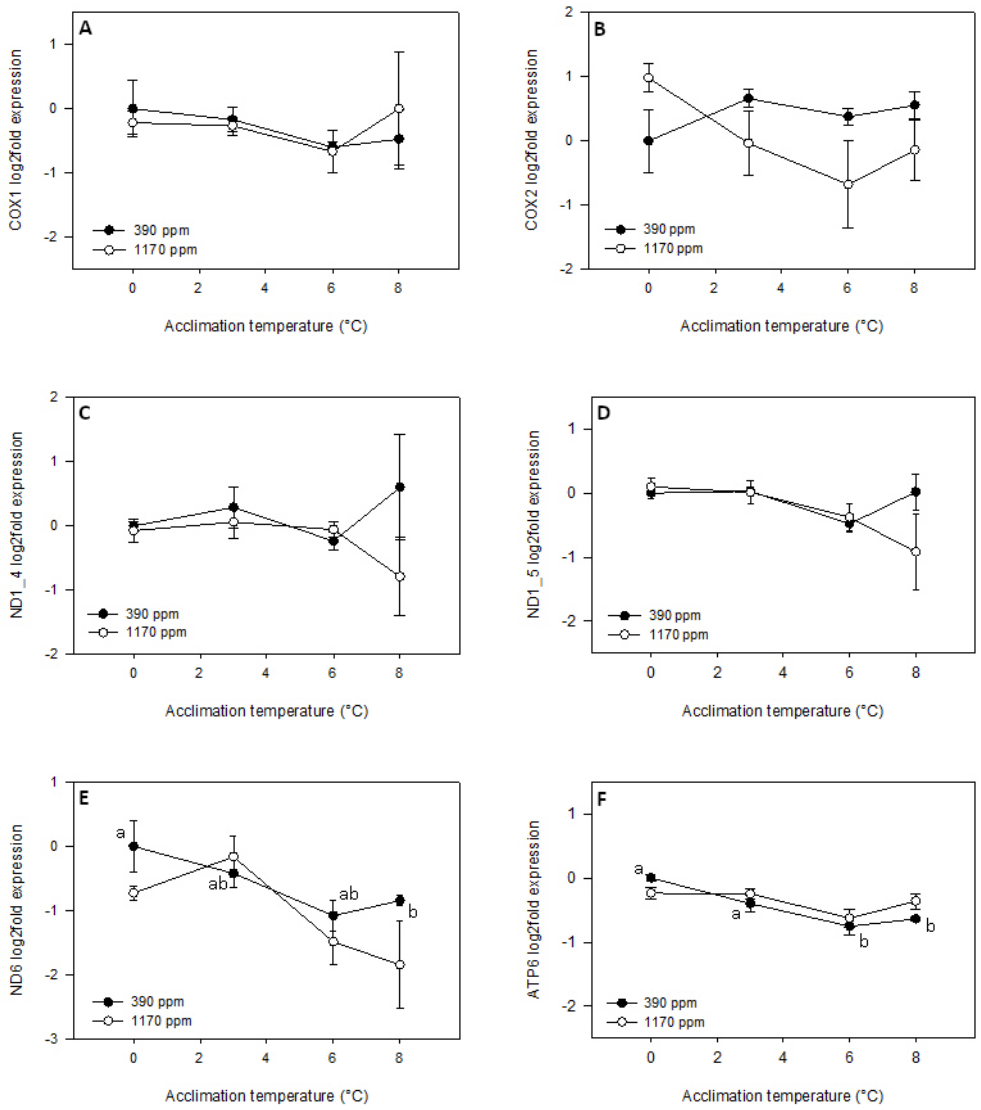

Figure 5.8 **mRNA log2fold expression of mitochondrial genes** of *B. saida* after 130 days of acclimation to a control condition (0 °C and 390 ppm) and to a combination of three elevated temperatures (3, 6, 8 °C) with control (390 ppm) and high pCO_2 (1170 ppm). The data were normalized to mean Ct values of Ubi and βAct. 0 °C, 390 ppm ppm pCO_2 was normalized to 0 (390 ppm: filled circles; 1170 ppm: open circles). A significant level of $\alpha = 0.05$ was chosen forANOVAway ANOVA. Significantly different groups are characterized by different letters, dots signed with *ab* represents intermediate groups, that are not significantly different from the others. The error bars display standard error.

5.4 Protein activity

5.4.1 Protein extraction optimization and protein content

Protein extractions for consecutive quantitative analyses like enzyme capacities or protein quantities have to be optimized for every species and tissue in any case to find the best compromise between maximum recovery, reproducibility and reliable results within the detection limits of the method. Lysis using a micro mill (Precellys) was not chosen as the final method despite good recovery because the extracts became cloudier than the lysates obtained from other methods making photometric measurements difficult. Moreover, in the act of transferring the lysate to a new tube, part of it was systematically lost. The homogenization via Ultra-Turrax presented the same problem, moreover part of the liquid was lost in the homogenization process, and the method was hence discarded. Hand homogenization alone proved to be more than efficient in lysing the tissue, as liver is a quite soft tissue without tough structures, and because the lysates obtained were much clearer. The upper lipid component after the centrifugation was elevated and its removal proved to be necessary before transferring the supernatant to a new tube.

Protein content steeply decreased with increasing temperature ($p < 0.001$) of almost a factor 2 (Figure 5.9). Hence, protein concentration significantly decreased until 6 °C, where its content stabilized. No pCO_2 effect was detected.

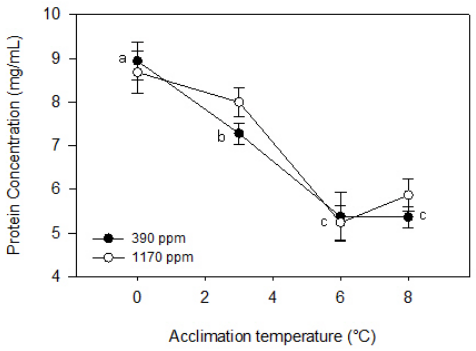

Figure 5.9 **Protein concentration in liver samples of *B. saida*** obtained via Bradford assay. Concentration is expressed as mg/mL and the error bars display standard error (390 ppm: filled circles; 1170 ppm: open circles). A significant level of $\alpha = 0.05$ was chosen for Two-way ANOVA.

5.4.2 Maximum cytochrome *c* oxidase activity

COX activities were normalized to the fresh weight. Both temperature ($p < 0.001$) and pCO_2 ($p = 0.015$) strongly influenced maximum COX activity (Figure 5.10, **A**).

Maximum activities increased more than 2fold between 0 and 6 °C ($p < 0.001$) with a significant drop between 6 and 8 °C ($p < 0.001$). Even though both factors affected COX activity, the interaction of temperature and pCO_2 was not statistically significant.

For the range 0-8 °C Q_{10} values for COX varied between 1.6 ± 0.1 and 1.4 ± 0.1 at 390 ppm and between 1.6 ± 0.1 and 1.2 ± 0.0 at 1170 ppm. COX Q_{10} significantly decreased with increasing temperature treatments ($p = 0.009$), but no effect of pCO_2 became apparent (Figure 5.10, **B**).

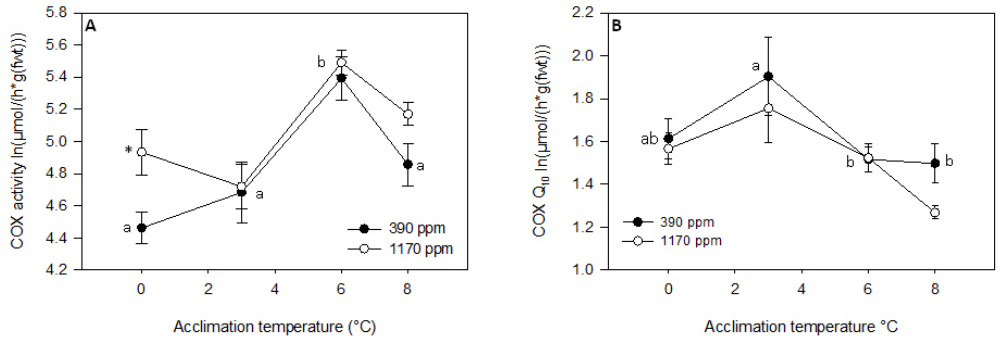

Figure 5.10 **Maximum COX activities and related Q_{10}.** Here are shown the activities measured at 0 °C assay temperature in relation to the fresh weight (**A**) and the temperature coefficient Q_{10} (**B**) obtained from the natural logarithm of individual activities measured at two assay temperatures, 0 and 10 °C (390 ppm: filled circles; 1170 ppm: open circles). A significant level of $\alpha = 0.05$ was chosen for Two-way ANOVA. Significantly different groups are characterized by different letters, dots signed with *ab* represents intermediate groups, that are not significantly different from the others. The error bars display standard error.

5.4.3 Maximum citrate synthase activity

CS activities were normalized to the fresh weight. CS activity was strongly influenced by rising temperature ($p < 0.001$) showing a steep decrease, and almost all temperature pairs showed a statistically significant difference. Nor pCO_2 neither temperature-CO_2 interaction effects became visible (Figure 5.11, **A**). A strong decrease in CS activity caused by rising temperature was highlighted with linear regression as well ($p < 0.001$).

Q_{10} values for CS varied for the range 0 -8 °C between 1.5 ± 0.05 and 0.9 ± 0.03 at 390 ppm and between 1.5 ± 0.07 and 0.9 ± 0.07 at 1170 ppm. Hence, a strong temperature-related decrease in the Q_{10} became apparent ($p < 0.001$), especially between 0 and the remaining acclimation temperatures (all $p < 0.001$) (Figure 5.11, B). No pCO_2 effects were visible.

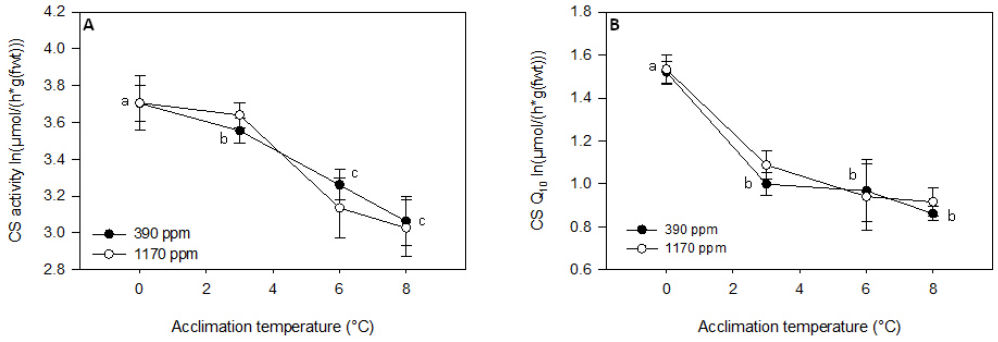

Figure 5.11 **CS maximum activity and related Q_{10}.** Here are shown the activities measured at 0 °C assay temperature in relation to the fresh weight (**A**) and the temperature coefficient Q_{10} (**B**) obtained from the natural logarithm of individual activities measured at two assay temperatures, 0 and 10 °C (390 ppm: filled circles; 1170 ppm: open circles). A significant level of $\alpha = 0.05$ was chosen for Two-way ANOVA. Significantly different groups are characterized by different letters. The error bars display standard error.

5.4.4 Protein expression of the F_OF_1 ATP synthase

Western Blot results are presented as the log2fold changes of the protein quantities referred to the fresh weight and normalized to the control conditions (0 °C, 390 ppm pCO_2). Before using any antibody for quantification, an evaluation of the specificity and the dynamic range for quantification needs to be done. Figure 5.12 demonstrates the high specificity of the heterologous F_OF_1 ATP synthase antibody originally raised against the respective protein from bovine, as only one band with the right molecular weight (about 55 kDa) could be detected. At higher concentrations a second, weak band at about 80 kDa arose, which might be due to some aggregation with other subunits of the protein complex. Thus, reliable detection of the fish F_OF_1 ATP synthase seems reasonable. To improve the dynamic range of quantitative detection BSA was supplemented to each lane. This approach turned out to be most successful, as the calibration curve displayed a linear increase over the entire range of concentrations. (Figure 5.13). Thus, the modified procedure turned out to be suitable for quantification of the F_OF_1 ATP synthase in liver extracts of *B. saida*.

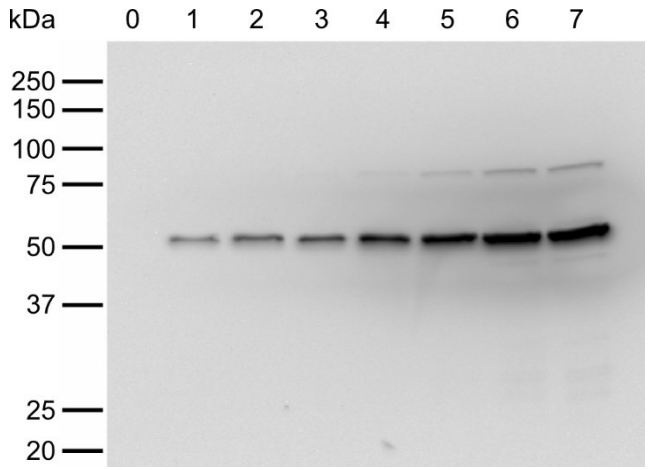

Figure 5.12 **Validation of antibody directed against bovine F_OF_1 ATP synthase.** The figure represents the membrane of an optimization test with 8 steps of a dilution series. Numbers of the top row (0, 1, 2, 3, 4, 5, 6, 7) correspond to the crude extract volume per lane (0, 0.25, 0.5, 1, 2, 4, 8, 10 µL).

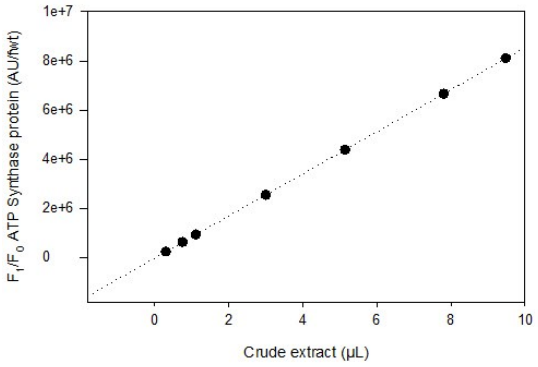

Figure 5.13 **Calibration curve** obtained during optimization of Western blot quantification. On the X axes the volumes of crude extract in each lane. On the Y axes the

The samples from all eight treatments were analysed according to the optimized protocol. F_OF_1 ATP synthase concentration, expressed as intensity (of the protein bands) per fresh weight, displayed a strong temperature-related decrease ($p = 0.018$), especially between 0 and 3 °C ($p = 0.017$) (Figure 5.14). This seemed to be slightly more pronounced for the control pCO_2, but pCO_2 had no significant effect upon Two-way ANOVA.

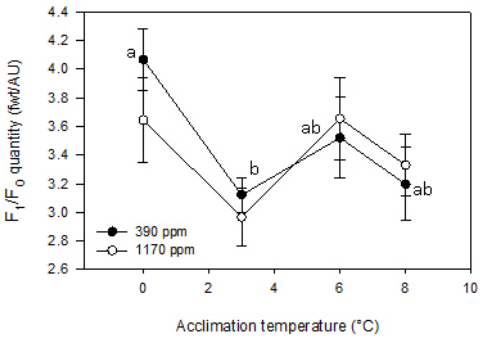

Figure 5.14 **Protein concentration in liver samples of *B. saida*** obtained via Western blot. Concentration is expressed as AU/*fwt* (390 ppm: filled circles; 1170 ppm: open circles). A significant level of $\alpha = 0.05$ was chosen. Significantly different groups are characterized by different letters, dots signed with *ab* represents intermediate groups, that are not significantly different from the others. Error bars display standard error.

6 Discussion

Human-driven climate change is affecting all ecosystems, hitting each one with different intensities. Polar systems are among the most affected, experiencing abrupt temperature changes with the related consequences, such as sea ice melting and reduced permanence of winter sea ice cover. As now, these changes will not reverse to a pre-industrialization condition, hence it is highly important to foresee and try mitigating further future damages. This study wants to offer additional aspects of *B. saida* response to rising ocean temperature and CO_2 concentration, to hopefully understand and help mitigate future losses in *B. saida* populations.

6.1 DNA expression and mitochondrial copy number

An important sentinel for cold compensation in ectotherms appears to be mitochondrial density, found to be higher in cold stenotherms and cold eurytherms (Johnston et al. 1998; Pörtner et al. 2008) and raised following cold acclimation (O'Brien 2011). This suggested an inverse pathway in the liver of *B. saida*, with a decrease in mitochondrial content with raising temperatures.

In this study, DNA expression of mitochondrial encoded genes was used as a proxy of mitochondrial copy number. As aforementioned, none of the 5 mtDNA encoded genes responded to acclimation temperature. Yet *nd1*, as well as the average mitochondrial genes (normalized to the mean C_T values of ND1_4, ND1_5, and ATP6) exhibited a significant downregulation when acclimated to control pCO_2 (390 ppm) and at 8 °C (Figure 5.5).The mitochondrial content of the liver of Polar cod was expressed as the mtDNA variation relative to nucDNA and was calculated as the geometrical mean of $2^{-\Delta\Delta Ct}$, where the ΔC_T represents the subtraction of the average C_T value of the target genes (ND1_4, ND1_5, ATP6,), chosen as endogenous control for their highly similar pattern (Figure 5.5), from the average C_T value of the control genes. The mtDNA copy number of liver cells of *B. saida* varied between 100 to 200 copies per nuclear haplotype, hence 200 to 400 copies per diploid cell, but were not significantly affected by temperature nor by pCO_2 acclimation (Figure 6.1), albeit a decrease between 6 and 8 °C can be noticed for both 390 ppm and 1170 ppm groups. These results match the data obtained by Hartmann et al. (2011), in whose study the mean mtDNA copy number per diploid cell ranged from 140 in gill of old animals to 1026 in liver of young animals of *Nothobranchius furzeri*. Moreover, a study by Battersby & Moyes (1998) found no significant change in mtDNA content expressed per total cellular DNA between cold and warm acclimated Rainbow trout (*Oncorhynchus mykiss*). Although

theoretically mitochondrial genes should follow the same pattern altogether, *cox1*, *cox2* and *nd6* display a diverse series of DNA expression. A possible reason may be that mtDNA is not replicated as a whole during the PCR procedure and just a mixture of fragments are replicated. This explanation works for *nd6*, which is located in the opposite strand, but not for *cox1* and *cox2*, that are located between *nd1* and *atp6*, thus, different stabilities of possibly fragmentated DNA may have influenced the outcome. Nonetheless, the pattern of *nd1* and *atp6* is the most consistent one and may thus represent the real situation. Certainly, more testing and possibly optimisation of the method is necessary.

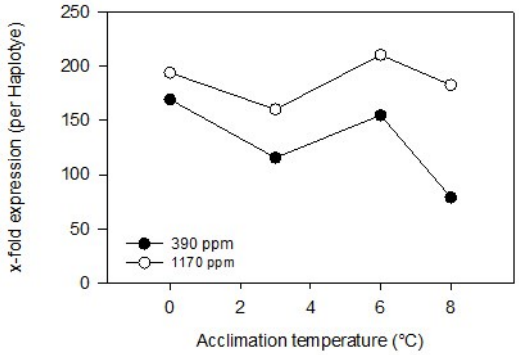

Figure 6.1 **Relative x-fold expression of *nd1* and *atp6* relative to the haplotype** of *B. saida* after 130 days of acclimation to control conditions (0 °C and 390 ppm) and to a combination of three elevated temperatures (3, 6, 8 °C) with control (390 ppm) and high pCO_2 (1170 ppm). The data were normalized to the mean C_T values of ND1_4, ND1_5, and ATP6 as endogenous control. 0 °C, 390 ppm pCO2 was normalized to 0 (390 ppm: filled circles, 1170 ppm: open circles). A significant level of $\alpha = 0.05$ was chosen for Two-way ANOVA.

NADH dehydrogenase subunit I has been widely mentioned in the literature as an appropriate endogenous control to determine mtDNA copy number (Longchamps et al. 2020; Grady et al. 2014; Jeng et al. 2007; Blokhin et al. 2008) also in fish (Li et al. 2023; Munro et al. 2019; Morgan et al. 2013). Hence, in this study ND1_4 and ND1_5 were used to measure mtDNA copy number along with ATP6 due to the highly similar DNA expression (see Figure 5.4, **C**, **D**, **G**).

In previous studies, CS activity was used as biomarker for mitochondrial density determination (Galgani et al. 2012; Larsen et al. 2012). In the present study, CS activity significantly decreases with the increasing acclimation temperature (Figure 5.11, **A**) and would henceforth support the hypothesis for which mitochondrial density is inversely proportional to acclimation temperature. Moreover, this decrease in activity matches the downward trend seen with *nd1* and *atp6* between

6 and 8 °C (Figure 6.1), however, certainly, more testing and possibly optimisation of the method is necessary to better align the different methods.

6.2 RNA extraction and optimization

Following RNA extraction, the purity of the nucleic acids was checked through Nanodrop. The mean 260/280 ratio is 2.08, with a minimum and maximum of 1.98 and 2.14, respectively; whereas the mean 260/230 ratio is 2.07 but oscillates between 0.64 and 2.48. Although the 260/280 ratio indicate high purity in all samples, the final recovery of the RNA from the silica column varied largely between specimens, resulting in huge variation of the 260/230 ratio, as buffer components dominate at 230 nm, if nucleotide concentration is low. Indeed, RNA qPCR results showed more variation than DNA results, mirroring the Shapiro-Wilk results: most of the normality tests resulted failed in the mRNA expression statistical analysis. Therefore, some of these results remain preliminary.

The same animals tested in the present study were used by Windisch et al (unpublished) for RNA extraction. The used method was phenol extraction by Trizol without a consecutive column-based purification. The final extracts present a higher RNA content, with similar 260/280 ratio of 2.08 (with a minimum of 2.02 and a maximum of 2.12) but a higher mean 260/230 ratio of 1.87 (with a minimum of 1.08 and a maximum of 2.31). The RNA integrity seemed to be slightly better according to the analyses by bioanalyzer. Anyway, Windisch et al. (unpublished) found a significant decrease of the RNA content caused by acclimation temperature and by the interaction between temperature and pCO_2, in line with the present study (Figure 6.2, **A**). Despite the possible differences in RNA purity and quality and the different extraction methods, in both cases a significant temperature-related reduction in the RNA concentration was found. Indeed, through linear regression, a significant correlation was found between the two differently extracted RNA samples ($p < 0.001$; Figure 6.2, **B**). As total RNA represents mostly the translation machinery, since about 90% of the total RNA corresponds to 18S and 28S rRNA, both extraction methods indicate a strong cold compensation of the translation system, or in this case, a reduction of surplus capacities in the warmth. This acclimatory response likely helps to avoid energy expenditure of costly cellular processes like protein translation and the consecutive protein synthesis.

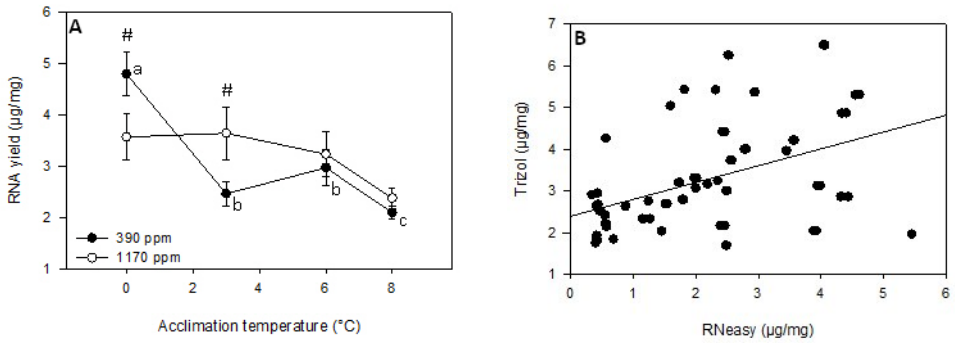

Figure 6.2 **RNA yield obtained by Windisch et al (unpublished)** with the same animals used in the present study (**A**) and correlation between the RNA concentrations obtained by the two RNA extraction methods (in the present study and in Windisch et al. unpublished, **B**). The RNA concentration was calculated through NanoDrop 2000/2000c Spectrophotometer analysis and is expressed as µg/mg. The error bars display standard error. A significance level of $\alpha = 0.05$ was chosen for Two-way ANOVA (390 ppm: filled circles, 1170 ppm: open circles). Significantly different groups are characterized by different letters and # represents the groups where a significant effect from the correlation between acclimation temperature and pCO_2 was detected.

6.3 Mitochondrial functioning after a long-term exposure

6.3.1 Citrate synthase

Citrate synthase represents a crucial enzyme, balancing both biosynthetic and oxidative pathways. CS operates in the mitochondrial matrix and is a key enzyme in the citric acid cycle, responsible for the synthesis of the citrate from acetyl-CoA and oxalacetate. Nonetheless, CS is a crucial component in the fatty acid final oxidation as well as lipid synthesis when acetyl-CoA in excess is shuttled from the mitochondrial matrix to the cytoplasm in the form of citrate (Windisch et al. 2011).

Table 6.1 **Summary of ANOVA results regarding citrate synthase analysis.** The signs + and - indicate a significant increase and decrease, respectively. 0 signifies absence of response.

Subunit	**DNA expression**		**RNA expression**		**Protein Expression**		**Enzyme capacities**		**Q_{10}**	
	Temp.	CO_2	Temp.	CO_2	Temp.	CO_2	Temp.	CO_2	Temp.	CO_2
CS	0	0	-	0			-	0	-	0

CS DNA expression presents itself as quite stable and no effects given by temperature nor pCO_2 were detected (Table 6.1, Figure 5.4, **B**). A significant downregulation was detected in mRNA expression of CS caused by increasing temperature and with its lowest expression at 8 C (Table 6.1, Figure 5.7, **B**). The mRNA downregulation caused a significant fall in the enzyme activity, which was

found to be sensitive to the increasing acclimation temperature (Table 6.1, Figure 5.11, **A**). This result contrasts with what Leo et al. obtained in 2020 with *B. saida* heart samples: CS activity was not affected by temperature, but by the high pCO_2 acclimation at relatively low temperatures (0 and 3 °C). Nonetheless, a pattern displaying an inverse relationship between CS activity and temperature was found here for liver CS capacities, bas has also been described in previous works: Batterby & Moyes (1998), Lucassen et al. (2003), and Lannig et al. (2003, 2005) found a significant increase in CS activity, as a form of cold compensation to low acclimation temperatures; while Battersby & Moyes (1998), Windisch et al. (2011), and Lannig et al. (2005) found a significant decrease in CS activity when the animals where acclimated to warm temperatures. Since in the latter case the Antarctic species presented a relative higher enzyme capacity than the temperate one (Lannig et al. 2005), it may be possible that this pattern is related to latitude and evolutionary cold adaptation.

Table 6.2 **Q_{10} values for the enzymes citrate synthase and cytochrome *c* oxidase.** Q_{10} means ± the standard deviations are shown in the table.

	Q_{10}	**Q_{10} 390 ppm**	**Q_{10} 1170 ppm**
COX	1.58 ± 0.34	1.63 ± 0.36	1.53 ± 0.31
CS	1.10 ± 0.35	1.09 ± 0.34	1.12 ± 0.36

The temperature coefficient Q_{10} is often employed in studies on enzymes as an indicator of thermal sensitivity (Clarke & Johnston 1999) as well as to detect a possible involvement of posttranslational mechanisms (Lucassen et al. 2003). Moreover, in some studies on ectotherms, Q_{10} reached 2 or more as a response to acute temperature change, indicating a high thermal activation of existing capacities, while after a chronic exposure to a non-optimal temperature, the Q_{10} would not overtake 1.5 resulting in less pronounced activities at high temperature (reviewed by Pörtner et al. 2006; Sandblom et al. 2014). In the present study, after a 4-month exposure to a combination of different temperatures and pCO_2 treatments, CS Q_{10} showed a significant temperature-related fall (Table 6.1; Table 6.2; Figure 5.11, **B**), with a mean Q_{10} of 1.5 ± 0.16 at 0 °C and 0.9 ± 0.15 at 8 °C (the values are presented as mean Q_{10} ± standard deviation). Similar results were obtained by Leo et al. (2020). The present results suggest that a posttranslational mechanism might have acted on CS activity as a result to increasing acclimation temperature. Moreover, CS seems to lose responsiveness with the long-term warm acclimation (at 8 °C Q_{10} is 0.89 ± 0.15). The contrary can be said for cold-acclimation, were CS Q_{10} value (1.53 ± 0.16 at 0 °C) indicates signs of cold-

compensation. Thus, on top of warm-reduced total capacities of CS (see above) post-translational adjustments seemed to be employed to avoid an overshot of activity under acute warming events. Together, CS seemed to be tightly regulated at several levels including transcriptional up to the post-translational levels. The question remains whether this response is within the thermal window of CS or the limited thermal flexibility after long-term exposure to 8°C indicates some level of stress of response limitation.

6.3.2 NADH dehydrogenase

The respiratory complex I or NADH dehydrogenase is an L-shaped protein complex located in the mitochondrial inner membrane, where it represents the entry point of the electrons in the electron transport chain (ETC). The complex I catalyses the oxidation of the NADH (Nicotinamide adenine dinucleotide) through the reduction of a ubiquinone (Q), present in its structure (reviewed by Hirst J. 2010). In this study two subunits of the NADH dehydrogenase were analysed, ND1 (for which two primer pairs were tested, ND1_4 and ND1_5) and ND6. Due to time constraints, only DNA and mRNA expression were measured. The DNA expression of *nd1* showed a significant downregulation caused by temperature and by pCO_2 acclimation, being the only significant change in DNA expression registered in all the analysed genes. Although *nd1* and *nd6* express for subunits of the same mitochondrial complex, the two do not present a similar DNA expression (see Table 6.3; Figure 5.5, **C**, **D**, **E**). Reasons for this discrepancy may be the location of the genes on the different strands of the mitochondrial genome and different distances to the origin of replication, but as discussed already above this needs to be investigated in more detail in future studies.

Table 6.3 **Summary of ANOVA results regarding NADH dehydrogenase analysis.** The signs + and - indicate a significant increase and decrease, respectively. 0 signifies absence of response.

Subunit	**DNA expression**		**RNA expression**		**Protein Expression**		**Enzyme capacities**		**Q_{10}**	
	Temp.	CO_2	Temp.	CO_2	Temp.	CO_2	Temp.	CO_2	Temp.	CO_2
ND1_4	0	-	0	0						
ND1_6	0	-	0	0						
ND6	0	0	-	0						

mRNA expression of the two genes was similar, hence both *nd1* (detected by ND1_5) and *nd6* significantly decreased following high temperature acclimation (see Figure 5.8, **C**, **D**, **E**). Although the downregulation was caused by acclimation temperature alone, and not by either pCO_2 nor the concomitant effect of the two, it is worth to notice that the graphs of ND1_5 and ND6 show a stronger decrease in

mRNA expression for the 1170 ppm group, of about 2fold and 4fold, respectively. Beside missing functional data, the warm-induced downregulation of two subunits of complex 1 indicates a similar compensation mechanism. Clearly, measurements of enzyme capacities and/or protein expression is necessary to characterise the outcome of the reduced mRNA expression.

6.3.3 F_OF_1 ATP synthase

F_OF_1 ATP synthase represents the final step for the electrons and exploits the proton flow generated by the ETC to produce ATP. This complex enzyme is composed by several subunits that can be grouped in two domains, F_O, or the *rotor*, located in the mitochondrial inner membrane, and F_1, or the *stator*, a hydrophilic structure that protrudes in the mitochondrial matrix. The protons flow, allowed through F_o, originates a torque able to rotate the two domains in opposite directions and generate three ATP molecules at the end of each revolution (reviewed by Elston et al. 1998).

Table 6.4 **Summary of ANOVA results regarding F_OF_1 ATP synthase analysis.** The signs + and - indicate a significant increase and decrease, respectively. 0 signifies absence of response.

Subunit	**DNA expression**		**RNA expression**		**Protein Expression**		**Enzyme capacities**		**Q_{10}**	
	Temp.	CO_2	Temp.	CO_2	Temp.	CO_2	Temp.	CO_2	Temp.	CO_2
ATP6	0	0	-	0	-	0				

In the present study the subunit ATP6, which belongs to the F_o complex, was analysed. The DNA expression of *atp6* was not significantly affected by the acclimation to the treatments, albeit a similar pattern as for *nd1* became visible for 6 and 8 °C for the 390 ppm treatment (Table 6.4; Figure 5.5, **F**). The mRNA expression was significantly reduced following the increase in temperature acclimation by a factor of about 2 (Table 6.4; Figure 5.8, **F**). Little is known about the effects of hypercapnia on the mRNA expression of the F_OF_1 ATP synthase. However, a study by Itoi et al. (2003) analysed the effects on different subunits of the two domains of the carp *Cyprinus carpio* when acclimated at 10 and 30 °C: the mRNA expression of all the F_OF_1 subunits analysed were significantly upregulated as a cold compensation to 10 °C acclimation in line with protein expression and functional capacities, indicating a tight transcriptional control. Here, reduced ATP6 mRNA expression aligned with significant 2fold downregulation of protein expression, which was mostly accentuated between 0 and 3 °C (Table 6.4; Figure 5.14). Thus, the F_OF_1 protein concentration may be regulated by the respective

mRNA following a long-term warm exposure similar to what has been found in the temperate carp.

Previous studies have found that lipids, particularly cardiolipin, can modulate mitochondrial enzymes capacity (Kraffe et al. 2007) and that inner membrane enzymes like complex I, complex IV and ATP synthase, are dependent on cardiolipin (reviewed by Schlame et al. 2000). Moreover, several studies have shown that lipid composition is modulated with thermal acclimation to keep a certain membrane fluidity at the respective temperature (so-called homeoviscous adaptation; reviewed by Hazel, 1995). Leo et al. (2020) found no variation in membrane lipid composition with increasing acclimation temperature in heart, in conjunction with decreased capacity of ETC related enzymes after acclimation to 8 °C. Therefore, the authors concluded the lack of homeoviscous adaptation with increasing temperatures might represents a weakness in the acclimation of *B. saida* at higher temperatures. In liver, reduced abundance of the F_OF_1 ATP synthase could be explained with an active regulation of transcript numbers. Again, a comprehensive picture on ATP synthase regulation and an involvement of posttranslational modifications would be given by the analyses on enzyme capacities, which could not be done here due to time-constraints. Furthermore, analyses of hepatic lipid composition would clarify the contribution of lipids on components of the respiratory chain.

6.3.4 Cytochrome *c* oxidase

Cytochrome *c* oxidase (COX) or Complex IV represents the last enzyme of the ETC. COX, a transmembrane enzyme located in the inner mitochondrial membrane, oxidises the cytochrome *c*, transferring the resulting electrons to molecular oxygen and producing water. At the same time, COX pumps protons into the intermembrane space, participating in the creation of the electrochemical potential to the mitochondrial matrix (reviewed by Michel et al. 1998).

Table 6.5 **Summary of ANOVA results regarding cytochrome *c* oxidase analysis.** The signs + and - indicate a significant increase and decrease, respectively. 0 signifies absence of response.

Subunit	**DNA expression**		**RNA expression**		**Protein Expression**		**Enzyme capacities**		**Q_{10}**	
	Temp.	CO_2	Temp.	CO_2	Temp.	CO_2	Temp.	CO_2	Temp.	CO_2
COX1	0	0	0	0			+	+	-	0
COX2	0	0	0	0						
COX4	0	0	-	0						

In this study, the DNA and mRNA expression of 3 subunits, COX1, COX2 and COX4, was analysed, yet no coherent results were obtained. The DNA expression of COX4, the nucDNA-encoded subunit, remains quite constant throughout the different treatments in line with the other investigated nuclear genes (Table 6.5; Figure 5.4, **A**). The two mtDNA-encoded subunits, COX1 and COX2, present varying DNA expression patterns among the treatments, which differ between the two, though no significant difference is present (Table 6.5; Figure 5.5, **A**, **B**). The reason for these discrepancies (as discussed above) remain open.

mRNA expression of *cox4* revealed a significant effect of temperature, which caused a 2fold downregulation, more pronounced in the 1170 ppm treatment (Table 6.5; Figure 5.7, **A**). Again, no coherent pattern was found with and between *cox1* and *cox2* mRNA expression, which were not affected by any treatment (Table 6.5; Figure 5.8, **A**, **B**). It is often assumed that changes in transcriptions explain changes in genes regulation, however, as this study witnesses, the subunits of the same enzyme can present different DNA and mRNA expressions, and these can even mismatch with the enzyme activity (Bremer & Moyes 2014). One explanation might be that most subunits mRNAs are in excess and only one is tightly regulated to control for the entire enzyme complex.

Unlike CS, COX maximum activity significantly increased by a factor of about 2 between 0 and 6 °C, thereafter it significantly dropped down at least under control pCO_2. This reversal was less pronounced for the high pCO_2 group at 8 °C. Additionally, a significant increase in activity was registered at 0 °C due to the high pCO_2 treatment (Table 6.5; Figure 5.10, **A**). Similar, Polar cod COX capacities in heart mitochondria measured by Leo et al. (2017, 2020) was significantly influenced by both temperature (Leo et al 2017, 2020) and pCO_2 acclimation (Leo et al 2020) and followed a bell-shaped thermal reaction norm with a maximum at 6 °C, and a decrease between 6 and 8 °C (trend not significant in Leo et a. 2017). Ultimately, the enzyme activity measured on the heart of *B. saida* by Leo et al. (2020) shows a significant decrease in COX activity and no response in CS activity following the interaction of high temperatures and pCO_2, and an overall low plasticity of the heart of *B. saida* to future climate change conditions. The Q_{10} value for COX decreased significantly between 3 and 8 °C (Figure 5.10, **B**) with a mean value of 1.6 ± 0.34 (the value is presented as mean Q_{10} ± standard deviation) (Table 6.2). A resemblance with the work of Leo et al. (2020) can be found, since the Q_{10} they measured was significantly affected by temperature, other than by pCO_2 acclimation. In a study by Kraffe et al. (2007) on the long-term warm acclimation of rainbow trout *Oncorhynchus mykiss* at 15 °C, although COX activity

significantly decreased, the Q_{10} value stayed between 1.4 and 1.6, a similar range of values obtained in the present work.

Thus, functional capacities and expression level of any investigated subunit did not align in the present study, the downregulation of *cox4* mRNA expression even followed an opposite trend. Higher translation efficiencies of reduced mRNA copies need to be postulated to explain higher capacities of the enzyme. As mentioned already above, none of the investigated subunits may limiting the transcriptional control of COX, but other, most likely nuclear-encoded subunits, may do so. The decrease in the Q_{10} can be interpreted as a sentinel for insensitivity of the enzyme to the raising temperature to avoid an overshot of existing capacities at higher, and possibly more fluctuating temperatures in the natural environment, as already discussed for CS. Together, our results indicate a strong participation of posttranscriptional and posttranslational regulation acting on COX, an explanation might be the higher translational efficiency of specific mRNA or changes in the rate of protein degradation, both hypothetically influencing the enzyme levels (Lucassen et al. 2003).

6.3.5 Metabolic shifts in mitochondrial functions

To provide some insights into possible shifts in mitochondrial functions the ratio of CS to COX was determined for each specimen separately. The CS-to-COX ratio significantly dropped by a factor of almost 3 with increasing acclimation temperature under both pCO_2 trials (Figure 6.3). Only at 0°C, a significantly higher ratio was detected under control pCO_2 compared to the other treatments. Investigations of CS and COX functions, two key enzymes of the citric acid cycle and ETC respectively, along with their ratio, has been widely used to monitor the long-term acclimation of fish mitochondria as well as tissue aerobic capacity (St-Pierre et al. 1998; Lucassen et al. 2006). Thus, the discrepancy between CS and COX activities might be explained by a relative increase in mitochondrial membrane over matrix functions (Lucassen et al. 2003; Vanderplancke et al. 2015; Ibarz et al. 2010). In the cold acclimated fish, the matrix over membrane ratio tends to increase, on the opposite, indicating higher CS capacities, which may be designated to lipid synthesis as a form of cold compensation (Paragraph 6.3; reviewed by Pörtner 2002 b; Lucassen et al. 2003).

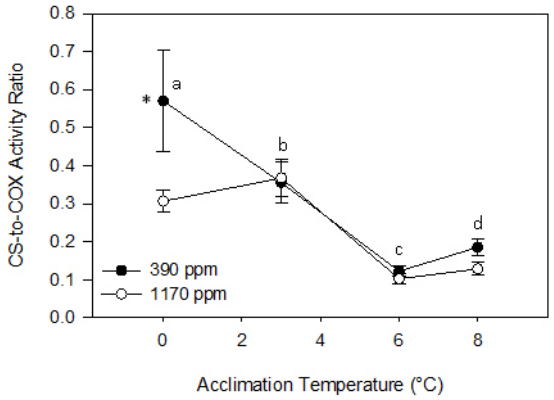

Figure 6.3 **Maximum CS-to-COX activity ratio.** Ratio of the maximum activity of CS and COX measured at 0 °C assay temperature obtained from the natural logarithm of individual activities measured at two assay temperatures, 0 and 10 °C (390 ppm: filled circles; 1170 ppm: open circles). A significant level of $\alpha = 0.05$ was chosen for Two-way ANOVA. Significantly different groups are characterized by different letters. * represents an effect of pCO_2 at the respective temperature. The error bars display standard error.

An increased activity of CS relative to COX supports the picture of lipid as preferred fuel to produce ATP, instead of carbohydrates in the cold. Hence, significant decrease in CS-to-COX ratio as well as increased activity in crucial enzymes in the β-oxidation have been registered in cold-adapted species such as Antarctic eelpout (*Pachycara brachycephalum*; Windisch et al. 2011), Antarctic plunderfish (*Harpagifer antarcticus*; Thorne et al.2010), exposed to warming, supporting this theory. Moreover, is well known that cold-adapted species show a preference towards fatty-acids metabolism rather than carbohydrates (Driedzic et al. 1996; Guderley & Gawlicka 1992; Sidell et al. 1995). Consequently, it has been postulated that due to its higher energy density, lipids are the preferred fuel for storage under normal conditions but needs to be replaced by carbohydrates under warm conditions as a kind of warm-hardiness (Windisch et al. 2011). According to the OCLTT concept (Pörtner et al. 2017; Pörtner & Farrell 2008) the likelihood of functional hypoxia increases with increasing temperatures. As the oxidation of lipids needs much more oxygen than carbohydrates, which can be even used under acute hypoxia, the preference of carbohydrates in the warmth may help the organisms to be prepared for such acute hypoxic conditions (Windisch et al. 2011).

Thus, the strongly decreasing ratio of CS to COX in *B. saida* under increasing temperature is in line with the beforementioned studies from temperate as well as cold-adapted fish and indicate a common mechanism of response to changing temperatures. Similar, a preferred use of carbohydrates relative to lipids in the warm can be postulated for hepatic mitochondria of *B. saida*. Moreover, high pCO_2 had a

similar effect on the ratio at low temperature, indicating a strong effect CO_2 on the use of fuels at natural habitat conditions. The implication of such a shift needs to be investigated.

However, the general increase in COX activity is not supported by ATP6 mRNA expression and, to a degree, by ND1 mRNA expression, subunits of genes related to the ETC. Although these discrepancies may be explained by altered transcriptional and posttranscriptional efficiencies and regulation similar to the investigated COX subunits, lower F_OF_1 ATP synthase protein expression followed the pattern of CS and not COX. Therefore, further studies on ATP synthase activity are needed to complete the picture.

6.4 Whole animal response

Even though *B. saida* is generally considered a polar stenotherm, the data collected through the years have originated a debate on whether Polar cod is a polar stenotherm or a cold eurytherm (Leo et al. 2017; Drost et al. 2016). On one hand, Polar cod in experimental condition have reached maximum cardio-respiratory capacity well over the range of temperatures they can experience in nature (Drost et al. 2016), as well as reaching T_{max} (temperature of maximum growth), S_{max} (swim activity with temperature up to a maximum), and condition factor at 7-8 °C when abundantly fed (Laurel et al. 2016). On the other hand, experimental conditions are not fully representative of the natural conditions in which *B. saida* lives (such as the abundance of food), and several studies have measured optimal growth at low and restricted temperatures windows for Polar cod (Laurel et al. 2016, 2017; Kunz et al. 2016), as well as mortality at 8 °C (Kunz et al. 2016).

The condition factor and hepatosomatic index (HSI) are often used to assess the overall health and well-being of the fish and their fluctuation can be caused by several reasons. In the present study, the HSI and the condition factor are both significantly affected by temperature and in opposite ways (Figure 5.1) as the first increases with increasing temperature, while the latter decreases. Despite matching with the result of Kunz et al. (2016), the trend they registered in HSI and condition factor were not significant. The significant decrease in the condition factor might represent the decline in health conditions caused by the increase in acclimation temperature. The same could not be hypothesized for HSI, seeing as usually this value increases in the cold-acclimated fishes, as instance in Lannig et al. (2003, 2005), and decreases in warm acclimated fish, as in Vergauwen et al. (2013) and Lannig et al. (2005). HSI, which represents the size of the liver relative to the whole organism size, reflects the organism energy status as lipids are stored in the liver

especially of gadid fish to large extent (Holdway & Beamish, 1984) and it seems logical that it follows the feeding state of the animals and parallels the data of the condition factor. The observed discrepancies between the two parameters may thus indicate that *B. saida* stores unused lipids in the liver at warm temperatures, which may serve as a reserve under more favourable conditions. This view is supported by the observed shift in mitochondrial functions, as the decreasing ratio of CS-to-COX may indicate the reduced use of lipids at the warm exposure temperatures. It needs to be deciphered, whether these metabolic shifts, observed under controlled laboratory conditions with optimal food supply, can be adopted in the environment.

6.5 Overview and conclusions

The results, now, together with the works of Kristina Kunz and Elettra Leo, need to be discussed in the light of the hypotheses proposed at the beginning of this master thesis (Paragraph 3.7).

The number of mitochondria significantly decreases as the temperature raises, with pCO_2 intensifying the temperature effect. The first hypothesis has to be rejected. On the one hand, some values conventionally correlated with mitochondrial density seems to corroborate the present hypothesis. As first is the significant temperature-related decrease in CS activity, which is considered a key mitochondrial enzyme and its activity a valid biomarker for mitochondrial density determination. No pCO_2 effect on CS activity has been measured. Leo et al. (2020) measured only a significant effect of high pCO_2 on CS activity. As second is the CS/COX ratio which can represent the ratio matrix-over-cristae ratio in the mitochondria. The significant decrease in the CS/COX ratio caused by temperature and pCO_2 acclimation, and the related decrease in matrix over cristae density, could be related to a decrease in the mitochondrial density, but also to a varying structure of individual mitochondria. Accordingly, the CS/COX ratio in Leo et al. (2020) showed a sensitivity to temperature acclimation. In the present thesis, mtDNA expression relative to representative nuclear genes was used for the first time to determine the mitochondrial density in *B. saida*. Besides some inconsistencies between the mitochondrial-encoded genes used, which needs to be ruled out in future studies, the results contrast with the value of the mtDNA expression, mitochondrial density biomarker chosen for the present study and highly used to determine mitochondrial density. The expression of the mtDNA, in relation to the nucDNA, was not affected by the acclimation to the treatments, even though a small effect of high pCO_2 on the DNA expression of the subunit ND1 was measured. Ultimately, notwithstanding the apparent lack in membrane lipids concentration change found by Elettra Leo in cardiac cells of *B. saida* following temperature increase, the present study data

support clearly a mitochondrial rearrangement in its structure and functions following the increase in temperature acclimation, with high pCO_2 having a small, but significant role in the mitochondrial response.

The raising temperatures cause a significant decrease in expression of the genes involved in the oxidative phosphorylation (*COX1, COX2, COX4, ND1, ND6, ATP6) and TCA cycle (CS), and high pCO_2 intensifies the temperature effect.* The DNA expression of the genes, which was tested in the present study as a proxy for mitochondrial copy number, was not sensitive to warm acclimation, only a significant decrease in expression caused by high pCO_2 is seen for ND1. The mRNA expression, on the other hand, seems to be more sensitive to temperature, especially of the subunits COX4, CS, ND6, ATP6. High pCO_2 does not affect mRNA expression. Given the present outcomes, it is possible to draw a pattern, according to that the raising temperatures significantly affects transcriptional mechanisms and possibly including higher degradation rates resulting in decreased abundance of the liver genes, or their subunits, involved in the oxidative phosphorylation and TCA cycle. This may indicate some sort of warm compensation, as higher transcriptional efficiencies from less mRNA copies may be assumed at warm temperatures. In line with this, the reduction in total RNA indicated a warm-compensated translation machinery, which may help to keep the energy budget balanced. High pCO_2 instead only seems to affect the DNA copy number of the mitochondrially-encoded genes, but only to less extent and at high temperatures. The exact mechanisms needs to be evaluated in future studies.

The enzyme function of and/or protein number of key mitochondrial components follow the responses at the mRNA level with high temperature and pCO_2 indicating a transcriptional regulation of mitochondrial functions. This hypothesis finds a confirmation with CS and ATP6, but not with COX, apparently. CS enzyme activity significantly decreases with increasing acclimation temperature, following the response of the mRNA expression; moreover, F_OF_1 ATP synthase protein expression is sensitive to temperature, matching the decline in mRNA expression of ATP6. COX enzyme activity, on the other hand, significantly increases with warm acclimation, contrasting not only the other enzymes pattern, but its mRNA expression as well. Nonetheless, the increase in COX activity stops at 6 °C, and after that it significantly and abruptly decreases at 8 °C: this behavior ultimately follows the optimal temperature curve for *B. saida*, defined by Kristina Kunz and Elettra Leo, with a maximum between 3 and 6 °C. In similar line, a significant temperature-related decrease in protein concentration (Figure 5.9) parallels these data as well as a significant temperature-related decrease in total RNA

concentration (Figure 5.6). Besides, the drop in Q_{10} for both, CS and COX, at warm temperatures indicate posttranslational modifications to be involved.

In conclusion, the long-term acclimation at high temperatures and pCO_2 shows a complex pattern of transcriptional and posttranscriptional regulation, including post-translational modifications on key mitochondrial enzymes in the liver cells of Polar cod, with consequent effect on the enzymes activity and expression. A reorganization in the mitochondrial properties and function is also evident. These results show a response in the acclimation process to the high temperature and pCO_2, and the liver of Polar cod seems to be more resilient than the heart. Nonetheless, the drastic fall of the temperature coefficient (Q_{10}) to almost 1 in both CS and COX is a sign of the loss of sensitivity of these key enzymes when acclimated to 8 °C, possibly a common mechanism to avoid an uncontrolled overshot of mitochondrial activity at fluctuating warm temperatures. In all this, temperature is the main driver of these changes, while pCO_2 acclimation seems to have a more marginal effect. Moreover, in addition to the physiological challenges *B. saida* might face with the imminent future scenario changes, the likely northward migration of the Atlantic cod (*Gadus morhua*), which shows higher plasticity and less constraints with the higher temperature and pCO_2 acclimation, will represents a threat to the survival of the Svalbard population of Polar cod, that might be outcompeted by Atlantic cod (Leo et al. 2017, 2020; Kunz et al. 2016).Ultimately, *B. saida* might not be able to thrive in 8 °C or even warmer waters for long periods.

7 Publication bibliography

Battersby B. J., Moyes C. D. (1998). Influence of acclimation temperature on mitochondrial DNA, RNA, and enzymes in skeletal muscle. *American Journal of Physiology* (*Regulatory, Integrative and Comparative Physiology*), 275, R905-R912. DOI: https://doi.org/10.1152/ajpregu.1998.275.3.R905.

Blokhin A., Vyshkina T., Komoly S., Kalman B. (2008). Variations in Mitochondrial DNA Copy Numbers in MS Brains. *Journal of Molecular Neuroscience*, 35, 283–287. DOI: https://doi.org/10.1007/s12031-008-9115-1.

Bouchard C., Fortier L. (2011). Circum-arctic comparison of the hatching season of polar cod *Boreogadus saida*: A test of the freshwater winter refuge hypothesis. *Progress in Oceanography*, 90, 105-116. DOI: https://doi.org/10.1016/j.pocean.2011.02.008.

Bradford M. M. (1976) A rapid and sensitive method for the quantitation of microgram quantities of protein utilizing the principle of protein-dye binding. *Analytical Biochemistry*, 72, 248-254. DOI: https://doi.org/10.1016/0003-2697(76)90527-3.

Breines R., Ursvik A., Nymark M., Johansen S. D., Coucheron D. H. (2008). Complete mitochondrial genome sequences of the Arctic Ocean codfishes *Arctogadus glacialis* and *Boreogadus saida* reveal oriL and tRNA gene duplications. *Polar Biology*, 31, 1245–1252. DOI: https://doi.org/10.1007/s00300-008-0463-7.

Bremer K., Moyes C. D. (2014). mRNA degradation: an underestimated factor in steady-state transcript levels of cytochrome c oxidase subunits?. *Journal of Experimental Biology*, 217, 2212-2220. DOI: https://doi.org/10.1242/jeb.100214.

Bulgin C.E., Merchant C.J., Ferreira D. (2020). Tendencies, variability and persistence of sea surface temperature anomalies. *Scientific Reports*, 10 (7986). DOI: https://doi.org/10.1038/s41598-020-64785-9.

Chung D. J., Schulte P. M. (2020). Mitochondria and the thermal limits of ectotherms. *Journal of Experimental Biology*, *223* (20). DOI: https://doi.org/10.1242/jeb.227801.

Clarke A., Johnston N. M. (1999). Scaling of metabolic rate with body mass and temperature in teleost fish. *Journal of Animal Ecology*, 68, 893-905. DOI: https://doi.org/10.1046/j.1365-2656.1999.00337.x.

Cohen D. M., Inada T., Iwamoto T., Scialabba N. (1990). Gadiform Fishes of the World (Order Gadiformes). An Annotated and Illustrated Catalogue of Cods, Hakes, Grenadiers and Other Gadiform Fishes Known to Date. *American Society of Ichthyologists and Herpetologists (ASIH)*, 10, 596-597. DOI: https://doi.org/10.2307/1446232.

Crawford R.E., Vagle S., Carmack E.C. (2012). Water mass and bathymetric characteristics of polar cod habitat along the continental shelf and slope of the Beaufort and Chukchi seas. *Polar Biology,* 35, 179–190. DOI: https://doi.org/10.1007/s00300-011-1051-9

David C., Lange B., Krumpen T., Schaafsma F., van Franeker J. A., Flores H. (2016). Under-ice distribution of polar cod *Boreogadus saida* in the central Arctic Ocean and their association with sea-ice habitat properties. *Polar Biology*, 39, 981–994. DOI: https://doi.org/10.1007/s00300-015-1774-0.

Doney S.C., Fabry V.J., Feely R.A., Kleypas J.A. (2009). Ocean acidification: the other CO2 problem. *Annual Review of Marine Science*, 1, 169-192. DOI: https://doi.org/10.1146/annurev.marine.010908.163834.

Driedzic W. R., Bailey J. R., Sephton D. H. (1996). Cardiac adaptations to low temperature in non-polar teleost fish. *Journal of Experimental Zoology Part A: Ecological Genetics and Physiology*, 275, 186-195. DOI: https://doi.org/10.1002/(SICI)1097-010X(19960601/15)275:2/3<186::AID-JEZ10>3.0.CO;2-I.

Drost H. E., Lo M., Carmack E. C., Farrell A. P. (2016). Acclimation potential of Arctic cod (Boreogadus saida) from the rapidly warming Arctic Ocean. *Journal of Experimental biology*, 219, 3114-3125. DOI: https://doi.org/10.1242/jeb.140194.

Elston T., Wang H., Oster G. (1998). Energy transduction in ATP synthase. *Nature*, 391, 510-513. DOI: https://doi.org/10.1038/35185.

Fang Y., Naik V., Horowitz L. W., Mauzerall D. L (2013). Air pollution and associated human mortality: the role of air pollutant emissions, climate change and methane concentration increases from the preindustrial period to present.

Atmospheric Chemistry and Physics, 13, 1377–1394. DOI: https://doi.org/10.5194/acp-13-1377-2013, 2013.

Galgani J. E., Johannsen N. M., Bajpeyi S., Costford S. R., Zhang Z., Gupta A. K., Ravussin E. (2012). Role of skeletal muscle mitochondrial density on exercise-stimulated lipid oxidation. *Obesity*, 20, 1387-1393. DOI: https://doi.org/10.1038/oby.2011.166.

Gleeson T.T. (1981). Preferred body temperature aerobic scope, and activity capacity in the monitor lizard, *Varanus salvator*. *Physiological Zoology*, 54, 423-429. DOI: https://doi.org/10.1086/physzool.54.4.30155835.

Grady J. P., Murphy J. L., Blakely E. L., Haller R. G., Taylor R. W., Turnbull D. M., Tuppen H. A. L (2014). Accurate Measurement of Mitochondrial DNA Deletion Level and Copy Number Differences in Human Skeletal Muscle. *PLOS ONE*, 9 (e114462). DOI: https://doi.org/10.1371/journal.pone.0114462.

Guderley H., Gawlicka A. (1992). Qualitative modification of muscle metabolic organization with thermal acclimation of rainbow trout, *Oncorhynchus mykiss*. *Fish Physiology and Biochemistry*, 10, 123-132. DOI: https://doi.org/10.1007/BF00004523.

Gundersen H. J. G., Bendtsen T. F., Korbo L., Marcussen N., Møller A., Nielsen K., Nyengaard J. R., Pakkenberg B., Sørensen F. B., Vesterby A., West M. J. (1988). Some new, simple and efficient stereological methods and their use in pathological research and diagnosis. *APMIS journal*, 96, 379-394. DOI: https://doi.org/10.1111/j.1699-0463.1988.tb05320.x.

Hardewig I., Van Dijk P., Moyes C., Pörtner H. O (1999). Temperature-dependent expression of cytochrome-c oxidase in Antarctic and temperate fish. *American Journal of Physiology*, 277, R508-516. DOI: https://doi.org/10.1152/ajpregu.1999.277.2.R508.

Hartmann N., Reichwald K., Wittig I., Dröse S., Schmeisser S., Lück C., Hahn C., Graf M., Gausmann U., Terzibasi E., Cellerino A., Ristow M., Brandt U., Platzer M., Englert C. (2011). Mitochondrial DNA copy number and function decrease with age in the short-lived fish *Nothobranchius furzeri*. *Aging cell*, 10, 824-831. DOI: https://doi.org/10.1111/j.1474-9726.2011.00723.x.

Hazel J. R. (1995). Thermal adaptation in biological membranes: is homeoviscous adaptation the explanation? *Annual review of physiology*, 57, 19-42. DOI: https://doi.org/10.1146/annurev.ph.57.030195.000315.

Hirst J. (2010). Towards the molecular mechanism of respiratory complex I. *Biochemical Journal*, 425, 327-339. DOI: https://doi.org/10.1042/BJ20091382.

Hochachka P. W., Somero G. N (2002). Biochemical adaptation: mechanism and process in physiological evolution. *Oxford university press*, 480 pages.

Holdway DA., Beamish FWH (1984). Specific growth rate and proximate body composition of atlantic cod (Gadus morhua L.). *Journal of Experimental Marine Biology and Ecology*, 81, 147-170. DOI: https://doi.org/10.1016/0022-0981(84)90003-0.

Hop H., Welch H. E., Crawford R. E. (1997). Population structure and feeding ecology of Arctic cod schools in the Canadian High Arctic. *Fish ecology in Arctic North America. American fisheries society symposium*, 19, 68-80.

Howald S., Cominassi L., LeBayon N., Claireaux G., Mark F. C. (2019). Future ocean warming may prove beneficial for the northern population of European seabass, but ocean acidification will not. *Journal of Experimental Biology*, 222 (21). DOI: https://doi.org/10.1242/jeb.213017.

Ibarz A., Blasco J., Gallardo M. A., Fernández-Borràs J. (2010). Energy reserves and metabolic status affect the acclimation of gilthead sea bream (*Sparus aurata*) to cold. *Comparative Biochemistry and Physiology Part A: Molecular & Integrative Physiology*, 155, 319-326. DOI: https://doi.org/10.1016/j.cbpa.2009.11.012.

Iftikar F. I., MacDonald J. R., Baker D. W., Renshaw G. M., Hickey A. J. (2014). Could thermal sensitivity of mitochondria determine species distribution in a changing climate? *Journal of Experimental Biology*, 217 (13). DOI: https://doi.org/10.1242/jeb.098798.

IPCC, 2014: Climate Change 2014: Synthesis Report. Contribution of Working Groups I, II and III to the Fifth Assessment Report of the Intergovernmental Panel on Climate Change [Core Writing Team, R.K. Pachauri and L.A. Meyer (eds.)]. IPCC, Geneva, Switzerland, 151 pp. (https://www.ipcc.ch/).

IPCC, 2023: Climate Change 2023: Synthesis Report. Contribution of Working Groups I, II and III to the Sixth Assessment Report of the Intergovernmental Panel

on Climate Change [Core Writing Team, H. Lee and J. Romero (eds.)]. IPCC, Geneva, Switzerland, 84. DOI: 10.59327/IPCC/AR6-9789291691647.

Itoi S., Kinoshita S., Kikuchi K., Watabe S. (2003). Changes of carp F_OF_1-ATPase in association with temperature acclimation. *American Journal of Physiology-Regulatory, Integrative and Comparative Physiology*, 284, R153-R163. DOI: https://doi.org/10.1152/ajpregu.00182.2002.

Jeng J. Y., Yeh T. S., Lee J. W., Lin S. H., Fong T. H., Hsieh R. H. (2007). Maintenance of mitochondrial DNA copy number and expression are essential for preservation of mitochondrial function and cell growth. *Journal of cellular biochemistry*, 103, 347-357. DOI: https://doi.org/10.1002/jcb.21625.

Jiang L. Q., Carter B. R., Feely R. A., Lauvset S. K., Olsen A. (2019). Surface ocean pH and buffer capacity: past, present and future. *Scientific Reports*, 9 (18624). DOI: https://doi.org/10.1038/s41598-019-55039-4.

Johnston I. A., Calvo J., Guderley H., Fernandez D., Palmer L. (1998). Latitudinal variation in the abundance and oxidative capacities of muscle mitochondria in perciform fishes. *Journal of Experimental Biology*, 201, 1-12. DOI: https://doi.org/10.1242/jeb.201.1.1.

Kraffe E., Marty Y., Guderley H (2007). Changes in mitochondrial oxidative capacities during thermal acclimation of rainbow trout *Oncorhynchus mykiss*: roles of membrane proteins, phospholipids and their fatty acid compositions. *The Journal of Experimental Biology*, 210, 149-165. DOI: https://doi.org/10.1242/jeb.02628.

Kunz K.L., Frickenhaus S., Hardenberg S., Johansen T., Leo E., Pörtner H. O., Schmidt M., Windisch H. S., Knust R., Mark F. C (2016). New encounters in Arctic waters: a comparison of metabolism and performance of polar cod (*Boreogadus saida*) and Atlantic cod (*Gadus morhua*) under ocean acidification and warming. *Polar Biology*, 39, 1137–1153. DOI: https://doi.org/10.1007/s00300-016-1932-z.

Laemmli, U (1970). Cleavage of Structural Proteins during the Assembly of the Head of Bacteriophage T4. *Nature*, 227, 680–685. DOI: https://doi.org/10.1038/227680a0.

Lannig G., Eckerle L., Serendero I., Sartoris F. J., Fischer T., Knust R., Johansen T., Pörtner, H. O. (2003). Temperature adaptation in eurythermal cod (*Gadus morhua*): a comparison of mitochondrial enzyme capacities in boreal and Arctic

populations. *Marine Biology*, *142*, 589-599. DOI: https://doi.org/10.1007/s00227-002-0967-6.

Lannig, G., Storch, D., Pörtner, H.O. (2005). Aerobic mitochondrial capacities in Antarctic and temperate eelpout (*Zoarcidae*) subjected to warm versus cold acclimation. *Polar Biology*, 28, 575–584. DOI: https://doi.org/10.1007/s00300-005-0730-9.

Larsen S., Nielsen J., Hansen C. N., Nielsen L. B., Wibrand F., Stride N., Schroder H. D., Boushel R., Helge J. W., Dela F., Hey-Mogensen M. (2012). Biomarkers of mitochondrial content in skeletal muscle of healthy young human subjects. *The Journal of physiology*, 590, 3349-3360. DOI: https://doi.org/10.1113/jphysiol.2012.230185.

Laurel B. J., Spencer M., Iseri P., Copeman L. A. (2016). Temperature-dependent growth and behavior of juvenile Arctic cod (Boreogadus saida) and co-occurring North Pacific gadids. *Polar Biology*, 39, 1127-1135. DOI: https://doi.org/10.1007/s00300-015-1761-5.

Laurel B. J., Copeman L. A., Spencer M., Iseri P. (2017). Temperature-dependent growth as a function of size and age in juvenile Arctic cod (Boreogadus saida). *ICES Journal of Marine Science*, 74, 1614-1621. DOI: https://doi.org/10.1093/icesjms/fsx011.

Leo E., Kunz K. L., Schmidt M., Storch D., Pörtner H. O., Mark, F. C. (2017). Mitochondrial acclimation potential to ocean acidification and warming of Polar cod (*Boreogadus saida*) and Atlantic cod (*Gadus morhua*). *Frontiers in Zoology*, 14, 1-12. DOI: https://doi.org/10.1186/s12983-017-0205-1.

Leo E., Graeve M., Storch D., Pörtner H. O., Mark F. C. (2020). Impact of ocean acidification and warming on mitochondrial enzymes and membrane lipids in two Gadoid species. *Polar Biology*, 43, 1109-1120. DOI: https://doi.org/10.1007/s00300-019-02600-6.

Li B., Wang H., Jiang C., Zeng X., Zhang T., Liu S., Zhuang Z. (2023). Tissue Distribution of mtDNA Copy Number And Expression Pattern of An mtDNA-Related Gene in Three Teleost Fish Species. *Integrative Organismal Biology*, 5 (1). DOI: https://doi.org/10.1093/iob/obad029.

Livak K. J., Schmittgen T. D. (2001). Analysis of Relative Gene Expression Data Using Real-Time Quantitative PCR and the $2^{-\Delta\Delta C_T}$ Method. *Methods*, 25, 402-408. DOI: https://doi.org/10.1006/meth.2001.1262.

Loeng H. (1991). Features of the physical oceanographic conditions of the Barents Sea. *Polar Research*, 10, 5-18. DOI: 10.3402/polar.v10i1.6723.

Longchamps R. J., Castellani C. A., Yang S. Y., Newcomb C. E., Sumpter J. A., Lane J., Grove M. L., Guallar E., Pankratz N., Taylor K. D., Rotter J. I., Boerwinkle E., Arking D. E. (2020). Evaluation of mitochondrial DNA copy number estimation techniques. *PLOS ONE*, 15 (e0228166). DOI: https://doi.org/10.1371/journal.pone.0228166.

Lucassen M., Schmidt A., Eckerle L. G., Pörtner H. O. (2003). Mitochondrial proliferation in the permanent vs. temporary cold: enzyme activities and mRNA levels in Antarctic and temperate zoarcid fish. *American Journal of Physiology-Regulatory, Integrative and Comparative Physiology*, 285, R1410-R1420. DOI: https://doi.org/10.1152/ajpregu.00111.2003.

Lucassen M., Koschnick N., Eckerle L. G., Pörtner, H. O. (2006). Mitochondrial mechanisms of cold adaptation in cod (*Gadus morhua* L.) populations from different climatic zones. *Journal of Experimental Biology*, 209, 2462-2471. DOI: https://doi.org/10.1242/jeb.02268.

McPhaden M. J., Zebiak S. E., Glantz M. H. (2006). ENSO as an integrating concept in earth science. *Science*, 314 (5806), 1740-1745. DOI: 10.1126/science.1132588

Michel H., Behr J., Harrenga A., Kannt A. (1998). Cytochrome *c* oxidase: structure and spectroscopy. *Annual review of biophysics and biomolecular structure*, 27, 329-356. DOI: https://doi.org/10.1146/annurev.biophys.27.1.329.

Michaelidis B., Spring A., Pörtner, H. O. (2007). Effects of long-term acclimation to environmental hypercapnia on extracellular acid-base status and metabolic capacity in Mediterranean fish *Sparus aurata*. *Marine biology, 150*, 1417-1429. DOI: https://doi.org/10.1007/s00227-006-0436-8.

Morgan J. A., Macbeth M., Broderick D., Whatmore P., Street R., Welch D. J., Ovenden J. R. (2013). Hybridisation, paternal leakage and mitochondrial DNA linearization in three anomalous fish (Scombridae). *Mitochondrion*, 13, 852-861. DOI: https://doi.org/10.1016/j.mito.2013.06.002.

Moyes C. D., Mathieu-Costello O. A., Tsuchiya N., Filburn C., Hansford R. G. (1997). Mitochondrial biogenesis during cellular differentiation. *American Journal of Physiology, Cell Physiology*, 272, C1345-C1351. DOI: https://doi.org/10.1152/ajpcell.1997.272.4.C1345.

Munro B., Horvath R., Müller J. S. (2019). Nucleoside supplementation modulates mitochondrial DNA copy number in the dguok$^{-/-}$ zebrafish. *Human molecular genetics*, 28, 796-803. DOI: https://doi.org/10.1093/hmg/ddy389.

O'Brien, K. M. (2011). Mitochondrial biogenesis in cold-bodied fishes. *Journal of Experimental Biology*, 214, 275-285. DOI: https://doi.org/10.1242/jeb.046854.

Otten A. B., Theunissen T. E., Derhaag J. G., Lambrichs E. H., Boesten I. B., Winandy M., van Montfoort A. P. A., Tarbashevich K., Raz E., Gerards M., Jo M. Vanoevelen, van den Bosch B. J. C., Muller M., Smeets H. J. M. (2016). Differences in strength and timing of the mtDNA bottleneck between zebrafish germline and non-germline cells. *Cell reports*, 16, 622-630. DOI: https://doi.org/10.1016/j.celrep.2016.06.023.

Ploumi C., Daskalaki I., Tavernarakis N. (2017). Mitochondrial biogenesis and clearance: a balancing act. *The FEBS journal*, *284*(2), 183-195. DOI: https://doi.org/10.1111/febs.13820.

Popov L. D. (2020). Mitochondrial biogenesis: An update. *Journal of cellular and molecular medicine*, 24, 4892-4899. DOI: https://doi.org/10.1111/jcmm.15194.

Pörtner H.O. (2002) (a). Climate variations and the physiological basis of temperature dependent biogeography: systemic to molecular hierarchy of thermal tolerance in animals. *Comparative Biochemistry and Physiology Part A: Molecular & Integrative Physiology*, 132, 739-761. DOI: https://doi.org/10.1016/S1095-6433(02)00045-4.

Pörtner H. O. (2002) (b). Physiological basis of temperature-dependent biogeography: trade-offs in muscle design and performance in polar ectotherms. *Journal of Experimental Biology*, 205, 2217–2230. DOI: https://doi.org/10.1242/jeb.205.15.2217.

Pörtner H. O., Bennett A. F., Bozinovic F., Clarke A., Lardies M. A., Lucassen M., Pelster B., Schiemer F., Stillman J. H. (2006). Trade-offs in thermal adaptation: the need for a molecular to ecological integration. *Physiological and Biochemical Zoology*, 79, 295-313. DOI: https://doi.org/10.1086/499986.

Pörtner H. O., Knust R. (2007). Climate change affects marine fishes through the oxygen limitation of thermal tolerance. *Science*, 315, 95-97. DOI: 10.1126/science.1135471.

Pörtner H. O., Bock C., Knust R., Lannig G., Lucassen M., Mark F. C., Sartoris F. J. (2008). Cod and climate in a latitudinal cline: physiological analyses of climate effects in marine fishes. *Climate research*, 37, 253-270. DOI: https://doi.org/10.3354/cr00766.

Pörtner H. O., Farrell A. P., (2008). Physiology and Climate Change. *Science*, 322, 690-692. DOI: 10.1126/science.1163156.

Pörtner H. O., Bock C., Mark F. C. (2017). Oxygen- and capacity-limited thermal tolerance: bridging ecology and physiology. *Journal of Experimental Biology 1*, 220, 2685–2696. DOI: https://doi.org/10.1242/jeb.134585.

Read C. C., Bhandari S., Moorey S. E. (2021). Concurrent measurement of mitochondrial DNA copy number and ATP concentration in single bovine oocytes. *Methods and Protocols*, 4, 88. DOI: https://doi.org/10.3390/mps4040088.

Rooney J. P., Ryde I. T., Sanders L. H., Howlett E. H., Colton M. D., Germ K. E., Mayer G. D., Greenamyre J. T., Meyer, J. N. (2015). PCR based determination of mitochondrial DNA copy number in multiple species. *Mitochondrial Regulation: Methods and Protocols*, 1241, 23-38. DOI: https://doi.org/10.1007/978-1-4939-1875-1_3.

Sabine C. L., Feely R. A., Gruber N., Key R. M., Lee K., Bullister J. L., Wanninkhof R., Wong C. S., Wallace D. W. R, Tilbrook B., Millero F. J., Peng T. H., Kozyr A., Ono T., Rios A. F (2004). The oceanic sink for anthropogenic CO2. *Science*, 305, 367-371. DOI: 10.1126/science.1097403.

Sandblom E., Gräns A., Axelsson M., Seth H. (2014). Temperature acclimation rate of aerobic scope and feeding metabolism in fishes: implications in a thermally extreme future. *Proceeding of the Royal Society B*, 281 (20141490). DOI: http://dx.doi.org/10.1098/rspb.2014.1490.

Schlame M., Rua D., Greenberg M. L. (2000). The biosynthesis and functional role of cardiolipin. *Progress in lipid research*, 39, 257-288. DOI: https://doi.org/10.1016/S0163-7827(00)00005-9.

Schurmann H., Christiansen J. S. (1994). Behavioral thermoregulation and swimming activity of two Arctic teleosts (subfamily *Gadinae*)-the polar cod

(*Boreogadus saida*) and the navaga (*Eleginus navaga*). *Journal of Thermal Biology*, 19, 207-212. DOI: https://doi.org/10.1016/0306-4565(94)90032-9.

Scott W. B., Scott M. G. (1988). Atlantic fishes of canada canadian bulletin of fisheries and aquatic science. 219.

Sidell B. D., Driedzic W. R., Stowe D. B., Johnston I. A. (1987). Biochemical correlations of power development and metabolic fuel preferenda in fish hearts. *Physiological Zoology*, 60, 221-232. DOI: https://doi.org/10.1086/physzool.60.2.30158646

Sidell B. D., Crockett E. L., Driedzic W. R. (1995). Antarctic fish tissues preferentially catabolize monoenoic fatty acids. *Journal of Experimental Zoology*, 271, 73-81. DOI: https://doi.org/10.1002/jez.1402710202.

Somero G. N. (2004). Adaptation of enzymes to temperature: searching for basic "strategies". *Comparative Biochemistry and Physiology Part B: Biochemistry and Molecular Biology*, 139, 321-333. DOI: https://doi.org/10.1016/j.cbpc.2004.05.003.

St-Pierre J., Charest P. M., Guderley H. (1998). Relative contribution of quantitative and qualitative changes in mitochondria to metabolic compensation during seasonal acclimatisation of rainbow trout *Oncorhynchus mykiss*. *Journal of Experimental Biology*, 201, 2961-2970. DOI: https://doi.org/10.1242/jeb.201.21.2961.

Stillman J. H., Somero G. N. (2000). A comparative analysis of the upper thermal tolerance limits of eastern Pacific porcelain crabs, genus *Petrolisthes*: influences of latitude, vertical zonation, acclimation, and phylogeny. *Physiological and Biochemical Zoology*, 73, 200-208. DOI: https://doi.org/10.1086/316738.

Strobel A., Leo E., Pörtner H. O., Mark F. C. (2013). Elevated temperature and PCO_2 shift metabolic pathways in differentially oxidative tissues of *Notothenia rossii*. *Comparative Biochemistry and Physiology Part B: Biochemistry and Molecular Biology*, 166, 48-57. DOI: https://doi.org/10.1016/j.cbpb.2013.06.006.

Thorne M. A. S., Burns G., Fraser K. P. P., Hillyard G., Clark M. S. (2010). Transcription profiling of acute temperature stress in the Antarctic plunderfish *Harpagifer antarcticus*. *Marine Genomics*, 3, 35-44. DOI: https://doi.org/10.1016/j.margen.2010.02.002.

Tronstad K. J., Nooteboom M., Nilsson L. I. H., Nikolaisen J., Sokolewicz M., Grefte S., Pettersen I. K. N., Dyrstad S., Hoel F., Willems P. H. G. M., Koopman

W. J. H. (2014). Regulation and quantification of cellular mitochondrial morphology and content. *Current pharmaceutical design*, 20, 5634-5652. DOI: https://doi.org/10.2174/13816128206661403052305 46.

Vanderplancke G., Claireaux G., Quazuguel P., Huelvan C., Corporeau C., Mazurais D., Zambonino-Infante J. L. (2015). Exposure to chronic moderate hypoxia impacts physiological and developmental traits of European sea bass (*Dicentrarchus labrax*) larvae. *Fish physiology and biochemistry*, 41, 233-242. DOI: https://doi.org/10.1007/s10695-014-0019-4.

Vergauwen L., Knapen D., Hagenaars A., De Boeck G., Blust R. (2013). Assessing the impact of thermal acclimation on physiological condition in the zebrafish model. *Journal of Comparative physiology B*, 183, 109-121. DOI: https://doi.org/10.1007/s00360-012-0691-6.

Watson R. T., Rodhe H., Oeschger H., Siegenthaler U. (1990). Greenhouse gases and aerosols. *Climate Change. The IPCC Scientific Assessment*, 1-40. Cambridge: Cambridge Univ. Press.

Welch H. E., Bergmann M. A., Siferd T. D., Martin K. A., Curtis M.F., Crawford R. E., Conover R. J., Hop H. (1992). Energy flow through the marine ecosystem of the Lancaster Sound region, Arctic Canada. *Arctic*, 45, 343-57. DOI: http://www.jstor.org/stable/40511483.

Windisch H. S., Kathöver R., Pörtner H. O., Frickenhaus S., Lucassen, M. (2011). Thermal acclimation in Antarctic fish: transcriptomic profiling of metabolic pathways. *American Journal of Physiology-Regulatory, Integrative and Comparative Physiology*, 301, R1453-R1466. DOI: https://doi.org/10.1152/ajpregu.00158.2011.

Windisch H. S., Frickenhaus S., John U., Knust R., Pörtner H. O., Lucassen, M. (2014). Stress response or beneficial temperature acclimation: transcriptomic signatures in A ntarctic fish (*Pachycara brachycephalum*). *Molecular ecology*, 23, 3469-3482. DOI: https://doi.org/10.1111/mec.12822.

Zanna L., Khatiwala S., Gregory J. M., Ison J., Heimbach P. (2019). Global reconstruction of historical ocean heat storage and transport. *Proceedings of the National Academy of Sciences*, 116, 1126-1131. DOI: https://doi.org/10.1073/pnas.1808838115.

8 Acknowledgements

Firstly, I would like to express my deepest gratitude to Prof. Chiara Papetti, an inspiring Professor and wonderful person, without whom this opportunity would not have been possible. I would like to thank her for her kindness and for always supporting me.

I am profoundly grateful to my tutor, Dr. Magnus Lucassen for giving me the chance to work on this remarkable project and for guiding me with diligence and patience. His constant encouragement along with our inspiring conversations made me open my mind on the physiology and molecular biology of fish. I would like to thank him for trusting in my skills and supporting me throughout the entirety of my work.

A special thanks to Dr. Felix C. Marks for the invaluable advice and for always having a kind word for me.

A special thanks to Anna Klitsch for her patience and kindness during the many hours we spent together in various laboratories.

This work would not have been possible without the support of the Integrative Ecophysiology team at AWI. I would like to profoundly thank you for your warm welcome and constant encouragement.

Finally, I would like to thank the most important people in my life: my parents for letting me follow my passions and make my dreams getting closer and closer; my two sisters that with unwavering support always stand by my side; my family for always being there for me; my boyfriend for the constant encouragement and for calling me “scientist”; and my best friends, my second family, for always motivating me since teenage years.